2-(mix)

D. E. Smith Code 553
8-16-72

Mechanism of Underthrusting in Southwest Japan: A Model of Convergent Plate Interactions

Thomas J. Fitch and Christopher H. Scholz

Lamont-Doherty Geological Observatory, Columbia University

Palisades, New York 10964

An elastic rebound mechanism consistent with underthrusting at the time of the magnitude 8.2 Nankaido earthquake of December 21, 1946 accounts for a reversal in sense between seismic and pre-seismic changes in elevation throughout a large portion of southwest Japan. This event and the magnitude 8.0 Tonankai earthquake of 1944 ruptured almost the entire boundary of the Asian and Philippine Sea plates between the Ryukyu and Izu-Bonin arcs. In terms of plate tectonics the formation of uplifted marine terraces ~~with~~ in the focal region of this earthquake can be explained by overriding of the Philippine Sea plate by the Asian plate as the former is consumed beneath southwest Japan. The absence of an inclined seismic zone, active volcanoes and a well-developed

101 pp

Need support ck acko

deep-sea trench suggests that underthrusting in southwest Japan started in geologically recent time, possibly less than one million years ago. However, an estimated slip rate of 8 ± 4 cm/yr suggests that typical island arc structures are rapidly evolving in this region. Similar seismic and pre-seismic movements within the focal regions on the 1960 Chilean and the 1964 Alaskan megathrusts, although based on comparatively little evidence, suggest that the inferred mechanism of underthrusting in southwest Japan is a reasonable model for interactions along other zones of plate convergence. Quasi-periodic recurrence of similar earthquake sequences in the past within each of these regions suggests that frequent monitoring of strain buildup can provide an improved measure of earthquake risk in these and other regions of underthrusting.

The fault motion during the 1946 Nankaido earthquake as inferred from geodetic data was predominantly, if not entirely, dip-slip. The rupture propagated almost 300 km southwest from the epicenter along an inferred strike of N70°E and extended well beyond the limits of the aftershock zone. The leading edge of the inferred fault is assumed to break the surface on the inner wall of the Nankai trough. In order to fit the data faults modeled as compound dislocations must be used. The preferred fault model is an underthrust dipping 30° to 40° toward the northwest. Slip calculated from a dislocation model increases from 5 to 18 meters in the direction of rupture propagation. Prior to the earthquake, from the 1890's to the 1930's strain increased at a constant rate. Following the earthquake a complex pattern of movements continued for about three years at rapidly decaying rates. These movements can be explained by reversed slip on nearly the entire fault surface that ruptured during the earthquake and by delayed forward slip on the deeper portions of the fault. Mechanically these movements are interpreted as a response to underdamped slip on shallow portions and overdamped slip on deeper portions of the fault surface at the time of the mainshock.

INTRODUCTION

The earth above the low velocity zone is divided into a number of large plates that in general move away from active ridges and toward island arcs [McKenzie and Parker, 1967; Morgan, 1968; Le Pichon, 1968; Isacks et al., 1968]. Although the gross motion of these plates on a time-scale of millions of years closely approximates rigid body motion [see e.g. Le Pichon, 1968] the seismicity within and on boundaries of these plates requires storage of elastic energy for periods of tens to hundreds of years, i.e., the time for the recurrence of most earthquakes of large magnitude. The release of elastic energy most often occurs near the frictional contacts between the major plates delineated by narrow zones of shallow earthquakes [see e.g. Barazangi and Dorman, 1969].

~~The release of stored elastic energy during~~ An earthquake is often thought of as an elastic rebound. The original rebound theory, illustrated in Figure 1A, was proposed by Reid [1910] to explain strike-slip movements on the section of the San Andreas fault that ruptured during the 1906 San Francisco earthquake. This theory, applied to strike-slip movements on a vertical fault, predicts that pre-seismic and seismic movements are anti-symmetrical with respect to the fault trace and that pre-seismic movements are opposite in sense to seismic movements. The sum of these movements is equivalent to a rigid translation of one side of the fault with respect to the other.

Movements inferred from several geodetic surveys that cross the

San Andreas fault zone support ~~the~~ elastic rebound theory. Horizontal movements accompanying several earthquakes located within this fault zone, the most famous of which is the San Francisco earthquake of 1906, fit displacement fields generated by fault models based on the theory of elasticity [Reid, 1910; Kasahara, 1958; Chinnery, 1961; Walsh, 1969]. Several sections of this fault zone have been surveyed during time intervals that do not include earthquakes of large magnitude [Whitten, 1948, 1955, 1958, and 1960; Hofmann, 1968]. Shear parallel to the fault zone inferred from these data is in general opposite in sense to shear released during earthquakes, as predicted by the theory. Scholz and Fitch [1969 and 1970] show that in general pre-seismic movements such as these are equivalent to movements generated by virtual slip in the opposite sense to the real slip that occurs at the time of the earthquake.

In this paper a rebound mechanism for underthrusting similar to that illustrated in Figure 1B is inferred from measurements of vertical and horizontal movements in southwest Japan associated with the 1946 Nankaido earthquake (Figure 2). These data, from repeated surveys during the last 100 years, are unique in that data of similar completeness are not now and will not in the near future be available for other regions of underthrusting. Such regions include the convex sides of most if not all active island arc and arc-like structures [Isacks et al., 1968], as inferred from numerous studies of earthquake mechanisms; Stauder and Bollinger [1964 and 1966a] for the Aleutian;

Isacks et al. [1969] for the Tonga-Kermadec; Molnar and Sykes [1969] for the middle America; Katsumata and Sykes [1969] for the Ryukyu; and Fitch [1970] for the Sunda and Philippine arcs. These regions of plate convergence and underthrusting contain the most active of the earth's seismic zones and include the focal regions of the largest known earthquakes such as the 1960 Chilean and 1964 Alaskan earthquakes [Plafker and Savage, 1970; Savage and Hastie, 1966; respectively]. Movements on large megathrusts such as these trigger most of the world's large tsunamis. Thus insight into the mechanism of underthrusting in southwest Japan contributes to a general understanding of source regions for some of the more wide-spread of natural disasters.

In contrast to most zones of underthrusting southwest Japan adjacent to the Nankai trough (Figure 2) does not have the structural features common to well-developed island arcs. Unlike the rest of Japan, this region did not become part of the late Cenozoic island arc system [Matsuda et al., 1967] that is still active in northeast Japan (Honshu island arc) adjacent to the Japanese trench (Figure 2) and in extreme southwest Japan (the northern end of the Ryukyu island arc). The deep and intermediate depth earthquakes beneath southwest Japan are not contiguous with the shallow seismicity paralleling the Nankai trough; instead they appear to lie within seismic zones that are inclined beneath the adjacent island arcs [see e.g., Katsumata and Sykes, 1969]. Southwest Japan also contrasts with typical island arcs by the absence of active volcanism as shown in Figure 2. However, in addition to the geodetic evidence for under-thrusting in this paper there is other evidence in this region for relative convergence between the Philippine Sea and Asian plates. Deformed sediments near the inner wall of the Nankai trough [Hilde et al., 1969] and two mechanism solutions from shallow earthquakes [Katsumata and Sykes, 1969] located beneath the adjacent continental slope are suggestive of a thrust contact between these plates.

Movements on opposite sides of the underthrust illustrated in Figure 1B, in contrast to movements generated by slip on a vertical fault, are not symmetrical by any relationship; although as in the case of slip on a vertical fault pre-seismic movements are opposite in sense to seismic movements. When comparing rebound mechanisms illustrated in Figure 1 it should be noted that the horizontal scale for the strike-slip movements is normally tens of kilometers (since seismic activity on nearly vertical faults such as the San Andreas is shallower than 20 km) while the scale for underthrusting is hundreds of kilometers.

The strike-slip and underthrusting sequences in Figure 1 are analogous sequences that obey rebound theory. Neither sequence is a complete tectonic model of faulting. For example underthrusting requires a sink for the underthrust material. In terms of plate tectonics the asthenosphere, a proposed layer of weakness relative to the overlying lithosphere [Isacks et al., 1968] acts as such a sink beneath convergent plate boundaries such as that inferred along the Nankai trough. Furthermore, it will be shown that simple underthrusting illustrated in Figure 1B must be modified to account for uplifted marine terraces within the focal regions of the 1946 Nankaido earthquake [see e.g., Watanabe, ~~1932; and Yoshikawa et al., 1964~~] and other recent megathrusts.

In a recent paper Mogi [1970] also recognized the consequences of underthrusting by a rebound mechanism. He showed that the net magnitude and direction of horizontal movements throughout Japan for approximately the last 50 years can be correlated with the occurrence or absence of major underthrusts on the inner walls of the Japanese trench and Nankai trough during that period. From the horizontal movements in southwest Japan (also discussed in this paper) he concludes that the 1946 Nankaido earthquake was a megathrust. Sugimura [personal communication] pointed out that Sawamura [1953 and 1954] proposed a similar mechanism to explain vertical movements within the focal region of this earthquake. However, he did not attempt to fit these data quantitatively to fault models as is done in this study.

Prior to this study vertical and horizontal movements at the time of two of the largest recorded earthquakes, the great Alaskan (1964) and the Chilean (1960) earthquake provided the most direct evidence for underthrusting of oceanic lithosphere [Savage and Hastie, 1966; Plafker and Savage, 1970; Hastie and Savage, 1970]. Within each focal region there was evidence for underthrusting from composite cross-sections of vertical movements generated at the time of the earthquake. In addition, horizontal movements in south - central Alaska provided conclusive evidence for a large component of thrust faulting during the 1964 earthquake [Parkin, 1969]. The only direct evidence for movements along the entire length of each rupture was uplift or subsidence of the shoreline. Geodetic data on pre- and post-seismic movements are totally lacking or at best sketchy for both focal regions; although geomorphological evidence shows that coastal regions of southeast Alaska subsided for hundreds of years prior to uplift at the time of the 1964 earthquake [Plafker and Rubin, 1967]. In general little is known of the mechanism of strain accumulation or the details of strain release in these regions.

In contrast to Alaska and Chile large areas of southwest Japan have been surveyed several times beginning with a leveling and triangulation survey in the late 1800's [Geographical Survey Institute of Japan, 1952, 1954, 1955 and 1967]. An extensive network of first order level lines was resurveyed three times in the last 100 years. In 1950 a second survey of the triangulation network was completed. In addition to the precise geodetic measurements mean-sea-levels were determined at tide gauge stations, some of which were in operation before 1900 [Hayashi, 1970]. Measured uplift and subsidence of coast lines is known for the latest Nankaido earthquake of 1946 as well as for those of 1707, and 1854. The seismic history of southwest Japan [Imamura, 1928; Kawasumi, 1951; Matuzawa, 1964] includes six seismic episodes since the 14th century that were similar to the activity in the mid-1940's, i.e., either a short series of regionally destructive earthquakes located on the continental slope or a single such event. The average recurrence time for these episodes is 118 ± 22 years. There are records of similar earthquakes from as early as the 7th century; however, the recurrence time for those events is nearly 200 years. The longer recurrence time may not be real, e.g., some events reported as only locally destructive may have been regionally destructive [see e.g. Imamura, 1928]. Coastal terraces resulting from similar earthquakes may be thought of as a record of paleoseismicity that in a crude sense can be traced back tens of thousands of years [Watanabe, 1932, 1948, 1959; Yoshikawa et al., 1964; Yonekura, 1968].

It will be shown that the seismic movements during the 1946 Nankaido earthquake were generated by slip on a complex thrust fault that is inferred to intersect the surface near the base of the continental slope. The pre-seismic deformation is explained by strain accumulation equivalent to a virtual dislocation with the same orientation as the fault surface but a sense opposite to that of the real dislocation that occurred at the time of the earthquake. Adjustments by slip along the fault surface and extensions of that surface can account for ~~the~~ post-seismic movements.

SEQUENCE OF MOVEMENTS AT MUROTO POINT

The sequence of movements related to the Nankaido earthquake of 1946 occurred in three distinct stages, a pre-seismic, seismic and post-seismic stage, each characterized by different rates of deformation. Throughout the terrestrial portion of the focal region there is evidence for such a sequence of movements; however, the tilting of Muroto Point (Figure 3) during the period from 1895 to 1953 [Nagata and Okada, 1947; Okada and Nagata, 1953] best illustrates the different stages of the earthquake sequence. Later in this paper profiles of pre-seismic and seismic movements across eastern Shikoku including Muroto Point and other parts of the focal region will show that the largest tilts within this region occurred along an imaginary curve paralleling the inferred strike of the rupture and passing close to Muroto Point. Thus Muroto Point is among the better locations within the focal region for measuring tilt.

Three leveling surveys completed in the period from 1895 to 1935 show that prior to the earthquake the point was gradually tilting toward the south at a constant rate. At the time of the Nankaido earthquake of 1946 an abrupt tilt was imposed on the point in a direction opposite to that of pre-seismic tilt. Following the earthquake there was a period of rapid recovery that lasted nearly three years. During this period about 20% of the tilt at the time of the earthquake was recovered.

The most recent Nankaido earthquakes prior to the one in 1946 were the well-documented summer and winter earthquakes of 1854 [Imamura, 1928]. These events resulted in uplift (and presumably a tilt in the northerly direction) at Muroto point of nearly the same magnitude as that which occurred in 1946 [Matuzawa, 1964]. If the recovery tilt was nearly the same following these earthquakes then the latest earthquake sequence resulted in a net or permanent tilt (the double headed arrow in Figure 4) of 1 to 2 sec in the same direction as the tilt at the time of the earthquake (i.e. in a northerly direction). Although the individual determinations of tilt between 1895 and 1935 are accurate to ± 0.01 sec [Okada and Nagata, 1953] the estimate of permanent tilt for the entire earthquake sequence can not be rigorously defended, chiefly because the assumed tilting during the previous earthquake sequence cannot be justified with certainty.

Uplifted marine terraces provide conclusive evidence for permanent deformation of this the southeastern peninsula of Shikoku [Watanabe, 1932, 1948, and 1959; Yoshikawa et al., 1964; Yoshikawa, 1970]. The oldest of these terraces may be 170,000 years old [Yoshikawa et al., 1964]. Each set of terraces has a northerly tilt as did the permanent tilt inferred from the latest earthquake sequence. In a later section the inflextion near the base of this peninsula between permanently uplifted and subsiding shorelines, i.e., the hinge line, is shown to coincide with a hinge line inferred from an estimate of net movement resulting from the latest earthquake sequence that includes the 1946 earthquake. In addition the rate of tilting for the entire peninsula is shown to be in reasonable agreement with rates inferred from the present tilts and estimated ages of the older terraces. These results support a generally accepted hypothesis that ~~the~~ permanent deformation of this and adjacent peninsulas evolved by intermittent tilts resulting from a series of Nankaido earthquakes that have recurred approximately once every 100 years for at least the last 100,000 years [Watanabe, 1932, 1948 and 1959; Yoshikawa et al., 1964].

THE 1946 NANKAIDO EARTHQUAKE

Introduction. Vertical movements generated at the time of the 1946 Nankaido earthquake are known from changes in shore lines, offsets in tidal records and differences in the relative elevation of bench marks surveyed before and after the earthquake. Differences in elevation between the new and old shoreline measured shortly after the earthquake are shown in Figure 5. Smoothed records from four tide gauge stations near the coast of Shikoku showed offsets (insets in Figure 5) at the time of the earthquake that agree within a factor of 2 with the less accurate measurements at the shoreline in the vicinity of each station. Reobservation of the leveling network ~~shown in~~ (Figure 3) within one year after the earthquake revealed vertical movements in a region nearly 200 km wide and 400 km long that are contoured in Figure 6. Peninsulas jutting into the Philippine Sea were uplifted while subsidence occurred in a broad zone between the peninsulas and central Honshu.

Absolute Datum for Vertical Movements. The contours in Figure 6 represent absolute changes in elevation from the time of the leveling survey carried out between 1928 and 1939 to the time of the first post-seismic survey completed one year after the earthquake. An absolute datum was determined for Shikoku by tieing the leveling data to the numerous measurements of uplift or subsidence of the shoreline and to the offsets in the tidal records shown in Figure 5. The error in the absolute datum is approximately 100 mm. The main sources of this error are the unavoidable inclusions of pre-seismic and post-seismic movements in the survey data for the earthquake.

Pre-seismic movements that probably continued from the time of the pre-earthquake survey to the time of the main shock are known to be in a sense opposite to movements that occurred at the time of the earthquake but much smaller in magnitude [Miyabe, 1955; Yoshikawa, 1970]. If tilt and vertical displacement are directly proportional, this error is between 13% and 5% of the true displacement at the time of the earthquake depending on the time of the pre-seismic survey. These estimates are based on the previously discussed linear rate for pre-seismic tilting at Muroto Point. The second main source of error, post-seismic movements, is difficult to evaluate; however, judging from the post-earthquake changes in mean-sea-level shown in Figure 5 this error is less than 10% of the actual earthquake displacement.

There are also errors in the shoreline measurements that by comparison with offsets in tidal records may be as large as 100%. However, it seems reasonable to assume that the shoreline measurements contain random errors but no large systematic errors. As a result this source of error is greatly reduced by using a large number of these measurements to determine the absolute datum. Nevertheless, errors in discriminating between subsidence due to local slumping and subsidence of the bedrock may be important in some regions where the coastline cuts alluvium.

The absolute datum for southwest Honshu and the Kii peninsula (Figure 3) was determined by assuming that bench mark 3028 near the Japan Sea coast of Honshu did not move during the period between surveys. This assumption seems justified because relative changes in elevation along this part of the coast varied less than $\pm$ 30 mm from 1927 to 1951 with bench mark 3028 and many other bench marks showing no relative movement. Data from a tide gauge station at Hamada near bench mark 3028 supports this assumption: Hayashi [1970] reports essentially no change in the height of local mean-sea-level at that station during this period. With this datum the maximum uplift at the tip of the Kii peninsula was 450 mm. This value is in reasonable agreement with a 375 mm drop in local mean-sea-level at Kusimoto (the tide station at the tip of this peninsula) relative to the nearest bench mark, for the period from 1930 to 1950 [Hayashi, 1970]. Changes in the shoreline were not used to determine an absolute datum for the Kii peninsula because only four of these measurements were found in the literature [Yonekura, 1968]; however, except for one data point on the east coast they are within a factor of two of absolute changes in elevation determined by assuming bench mark 3028 stationary. Although data from level-lines connecting the network in southwest Honshu with that in Shikoku (Figure 3) were not available for this period, the inferred ~~change in amount of~~ subsidence between the islands is consistent with a continuous decrease in subsidence in a northerly direction.

Dislocation Model and Fault Parameters. The field of vertical displacements represented by the contours in Figure 6 is similar to vertical displacements generated at the times of the Chilean (1960) and Great Alaskan (1964) underthrusts [Savage and Hastie, 1966; Plafker and Savage, 1970; Plafker, 19~~70~~69]. The direction of horizontal movements within the focal region which will be discussed later precludes either slip in the sense of high-angle thrust faulting or slip with a large strike-slip component. It will be shown that vertical as well as horizontal movements at the time of the Nankaido earthquake are closely approximated by displacement fields generated by elastic models for underthrusting. These models come from a class of theoretical elastic dislocations in which the discontinuity in displacement across the dislocation surface is restricted to a pure translation [Love, 1944; Steketee, 1958; Maruyama, 1964]. Convenient equations for ~~the~~ displacement fields generated by these dislocations were ~~have been~~ derived by Mansinha and Smylie [1970] and are ~~were~~ used in this study. Their equations are equivalent to those derived by Savage and Hastie [1969].

The fault parameters needed to define this megathrust are those parameters defining the position in space and the size of the fault surface, which as a first approximation is assumed to be a plane, and the amount of slip on that surface. The position in space is determined by the strike, dip and the location of at least one point on the fault surface with respect to a geographic coordinate system. The size is determined by the length of the rupture along strike and the down-dip length of the fault.

Solutions to the measured field of vertical displacements for the 1946 Nankaido earthquake using models for buried faults indicate that the leading edge of the thrust could be buried to a depth of at most a few tens of kilometers. However, data near the leading edge needed to give firm evidence for a buried fault do not exist. Thus within an uncertainty of a few tens of kilometers the fault is assumed to have reached the surface. Evidence from echograms for several offsets in near surface formations is consistent with thrust faulting on the lower reaches of the continental slope [Hilde et al., 1969]; however, it is not possible to determine which if any of these offsets corresponds to movement at the time of the 1946 Nankaido earthquake.

The surface that ruptured during this earthquake is assumed to have the same strike, N70°E, as the Nankai trough; a topographic depression similar to deep-sea trenches that are often identified with boundaries between converging plates of lithosphere. The assumed strike is consistent with the east-west trend in the field of vertical displacements shown ~~contained~~ in Figure 6. Furthermore, a preliminary focal mechanism for the Nankaido earthquake [Kanamori, personal communication] is consistent with thrust faulting on a plane with a shallow northward dip and approximately this strike.

The southwestern end of the thrust is defined by the abrupt change in strike of displacement contours in west-central Shikoku (Figure 6). From the leveling data the extent of faulting in the northeast direction is uncertain because the Tonankai earthquake with a magnitude of 8.0 [Matuzawa, 1964] occurred east of the Kii peninsula in 1944 (Figure 3) and may have contributed much of the displacement in that region. The M = 7.5 Mikawa earthquake of 1945, whose epicenter is shown in Figure 3, also occurred between the two surveys, but Hatori [1970] showed that displacements generated at the time of this event did not contribute to the measured displacements on the Kii peninsula. However, a well-defined boundary, shown in Figure 7, exists between the aftershock zones of the Nankaido and Tonankai earthquakes. This boundary is taken as the northeastern end of the Nankaido rupture. From this evidence the fault length of 280 km for the 1946 Nankaido earthquake may be accurate to within a few tens of kilometers and is in reasonable agreement with a length of 350 km for the tsunami-generating region [Omote, 1947; Hatori, 1966].

For the purpose of fitting the leveling data from the Kii peninsula and Shikoku to displacements generated by a single fault the Nankaido rupture is extended 60 km toward the northeast. The resulting hybrid fault, which will include part of the Tonankai as well as all of the Nankaido earthquake, is 320 km long. A fault with this length is used in all the computations.

The remaining variables needed to define the rupture are fault dip, slip, down-dip length and the position of the fault trace in the direction normal to the strike. Applying an optimization technique to determine the best values for these variables is impossible because the measured displacement field (Figure 6) has strong gradients in directions parallel as well as perpendicular to the strike of the fault. The gradient parallel to the strike is such that the zone of subsidence, contoured by dashed curves in Figure 6, becomes markedly more pervasive toward the western end of the focal region. As a result contours are deformed into sinuous curves; e.g., the contours near the southern coast of Shikoku are rotated as much as 30° toward the south between the eastern and western ends of the island. Such a field is not closely approximated by uniform slip on a rectangular surface. Realistic fault models must be compound rather than simple dislocations. Thus one must use a trial and error procedure to find acceptable models.

To minimize the uniqueness problem inherent in a trial and error procedure a range for each of the variables was estimated by fitting, in a least-squares sense, portions of the measured displacement field to fields generated by simple dislocations; e.g., uniform slip on rectangular surfaces. The displacement fields within regions A and C (Figure 3); e.g., eastern and west-central Shikoku, respectively, were used for this purpose. Region A was chosen because this is the region closest to the northeastern end of the Nankaido rupture for which the measured displacement field is not contaminated by movements at the time of the Tonankai earthquake. Region C was chosen because in this region the subsidence reached a maximum for the entire focal region.

Tables I and II give the solutions for the displacement fields within Regions A and C respectively. The better solutions are those with standard deviations between measured and computed displacements that are close or coincide with the minimum deviation, which for Region A is nearly 70 mm and for Region C is nearly 50 mm. The corresponding solutions to displacements in Regions A and C are thrusts that dip 30° to 45° and 30° to 40° toward the NNW. In Table II the model of a fault with a dip of 20° is considered unreasonable, because the corresponding position of the fault trace given by parameter R is seaward of the Nankai trough. It is apparent from the other solutions given in the tables that an increase in standard deviation by 10 mm is considered large enough to exclude that solution from the group of better solutions. The significance of such a small increase can not be rigorously defended and may not be important. Slip, which is clearly the least well-determined of the fault parameters, is the only parameter that is greatly affected by including one or two additional solutions in the group of better solutions. The slip for the better solutions varies by as much as a factor of 3, while the down-dip length of the fault remains nearly constant.

Fault Models. Two trial and error solutions to the measured field of vertical displacements (Figure 6) are illustrated in Figure 8. These models were obtained by dividing the fault surface into five or six rectangular sections along strike and using the better solutions to profiles A and C as guides for choosing the initial values for the fault parameters in each section. The initial model was then refined by adjusting the width and length of each section as well as the slip. For Model A the northeast part of the fault has a dip of 40° and the southwest part has a dip of 30°. From northeast to southwest the slip increases from 5 to 18 meters. The down-dip length of the fault varies from 50 km in that portion of the fault that slipped the least to 130 km in that portion of the fault that slipped the most. Model B is similar to Model A except that the dip is held constant at 35°. As a result the slip varies by a factor of 8 from one end of the fault to the other. Model A is preferred because within the acceptable range of the variables (dip, slip, down-dip length and position normal to strike) this model minimizes the gradient in slip. Models A and B have moments of 7.8×10^{28} and 9.0×10^{28} dyne cm, respectively, that are within a factor of 2 of the seismic movement estimated by Brune and Engen [1969] for a shallow earthquake of the dip-slip type with magnitude 8.2.

Figure 9 shows the field of vertical displacements generated by Model A. Model B generates approximately the same field on terrestrial portions of this region. A comparison with Figure 6 shows that the generated field has very closely the same shape as the measured field; however, there are local differences as large as 150 mm between the measured and computed fields, particularly along the southern coast of Shikoku where the gradients are large. The down-dip length of the fault controls the position of the inflection between uplift and subsidence; ~~i.e., the hinge line;~~ thus it is possible, as in Model B, to deform the hinge line into a sinuous curve and still keep the fault surface planar.

Figure 7 shows that the rupture propagated mostly unidirectionally toward the southwest and extended beyond the southwest limit of the mapped aftershock zone. The relocated epicenter for the main shock (Figure 7) of 33.14°N and 135.85°E confirms the unidirectional character of the rupture. The recomputed depth of focus was 32 km which is about 20 km deeper than the depth predicted from Model A for the same epicenter. This discrepancy is easily within the uncertainty of the seismically determined focal depth. Aftershocks reported in the ISS (International Seismic Summary) for the first month after the main shock were also relocated (Figure 7). They confirm the size of the aftershock zone for this period reported by Mogi [1968]. The aftershock zone in the following months did not significantly extend itself toward the southwest [Utsu, 1957; Mogi, 1968]. Thus the zone of aftershocks did not extend to that portion of the fault that slipped the most.

To complete this argument it ~~is necessary to show that vertical~~ movements outside the aftershock zone cannot be explained by slip acting over a much reduced fault surface defined by the aftershock zone. In general strike-slip generates large vertical movements near the ends of the rupture [see e.g., Chinnery, 1961]. Such a component in the right-lateral sense acting over that portion of the inferred megathrust beneath the aftershock zone could account for a significant portion of the subsidence in western Shikoku; however, well-documented uplift of the eastern coast of the southwest peninsula of Shikoku, including Ashizuri point (Figure 3), is conclusive evidence against this possibility. This uplift is known from sea levels ~~tidal records,~~ recorded at a local station, and from changes in the shoreline following the earthquake [see e.g. Matuzawa, 1964]. If ruptures in other regions of underthrusting extend beyond their aftershock zones, small gaps (e.g., gaps less than 200 km) between aftershock zones cannot with confidence be used as evidence for an impending earthquake in such regions.

Horizontal Movements. Underthrusting with the parameters of Model A generate horizontal displacements of about 1/2 meter on the Japan Sea coast of southwest Japan (Figure 10). Only the component perpendicular to the strike of the fault is contoured because within the contoured region this component is larger by about one order of magnitude than the component parallel to the strike. Also shown in Figure 10 are adjusted magnitudes ~~nitudes~~ of horizontal displacements computed from triangulation data [Geogr. Surv. Inst. of Japan, 1952]. Because the first triangulation survey was completed 47 years before the earthquake, and the second was completed three years after the earthquake, the resulting displacement field is seriously contaminated by post- as well as pre-earthquake movements. To adjust for a bias resulting from the inclusion of pre-seismic movements, magnitudes of horizontal displacement computed from triangulation data were multiplied by 2.2. This factor comes from the following ratio based on leveling data from the southeastern peninsula of Shikoku (to be discussed later):

$$\frac{\text{Tilt at the time of the earthquake less 6 months of reversed tilt after the earthquake}}{\text{Net tilt from 1894 to 1949 (the average period between the two triangulation surveys)}}$$

The six months of reversed tilt in the numerator is included to adjust for the fact that the first post-seismic survey of the leveling network was completed on the average six months after the mainshock, and, consequently the dislocation models were computed to displacements which included this movement. Even with this correction the adjusted displacements are systematically smaller than the displacements generated from the fault model. This discrepancy can be explained at least qualitatively by movement of the base line at the time of the earthquake as indicated in Figure 10. The inferred displacement of the southern end of the base line is nearly 2 meters in a southernly direction while the north end of the line moved about 0.5 meter in the same direction. Thus the line was stretched as well as translated. The translation of the line is in the correct sense to yield underestimates of the real displacement field. A quantitative correction for this movement is impossible unless a new base line can be established for which the assumption of stationarity is more likely to be fulfilled.

In Figure 11 directions of horizontal displacements computed from the triangulation data are compared with directions computed from Model A. The mean direction from survey data is S30°E and the standard deviation is within 10° of the normal to the Nankai trough and to the inferred strike of the megathrust. It is not known how much this result is influenced by the choice of the fixed base line. However, aside from data points near the fixed line (most of which are not shown in Figure 10) there are no obvious systematic changes in direction as a function of position within the focal region.

Directions computed from Model A with few exceptions are in reasonable agreement with directions computed from the survey data. In western Shikoku the displacement vectors from Model A are rotated by as much as 30° in a counterclockwise sense from the normal to the fault trace. This rotation is an end effect of thrust faulting and may in part account for a similar trend in the directions observed in the survey data. In the southeastern part of the Kii peninsula the directions from Model A are nearly perpendicular to the strike of the megathrust and as much as 30° in a clockwise sense from directions computed from survey data. It is possible that this discrepancy is the result of systematic errors in the triangulation data. The stations in southern Kii are not well controlled in the southern and eastern quadrants. It is also possible that displacements at the time of the Tonankai earthquake in 1944 generated horizontal displacements that in this region had a southeasterly strike. In any case the directions computed from the survey data strongly suggest that most if not all of the motion resulted from thrust faulting. However these data are not accurate enough to preclude a small strike-slip component. If such a component in the right lateral sense did exist it would have to be confined to the eastern part of the fault because uplift near Ashizuri point (Figure 3) is completely incompatible with even a small right lateral component. For example a right lateral component that is 15% of the dip-slip component in Model A would generate approximately one meter of subsidence near Ashizuri point.

PRE-SEISMIC, SEISMIC AND POST-SEISMIC MOVEMENTS

Introduction. As already shown, displacement fields computed from elastic dislocation models of faulting can successfully describe vertical and horizontal movements generated at the time of an earthquake. ~~These~~ Computed displacement fields can also describe movements generated by slip that may take place during periods of time that are long in comparison with the time for the propagation of the initial rupture. Such slip may or may not trigger the release of seismic energy. For example, episodes of "slow slip" or creep were triggered by the 1966 Parkfield earthquake in central California [Scholz et al., 1969] and the 1968

Borrego Mountain earthquake in southern California [Hamilton, in preparation]. Post-seismic movements on a much larger scale were triggered by the 1946 Nankaido earthquake. These movements can be explained by slip in the forward and reverse sense on different portions of a fault surface that includes the surface that ruptured during the mainshock. Moreover, pre-seismic movements in the focal region of this earthquake that are consistent with strain buildup on a "locked" fault (illustrated in Figure 1B) can be explained by slip (in this case virtual slip) on a fault surface with nearly the same dimensions as that which ruptured during the mainshock.

Virtual slip computed for a period of strain buildup is simply the amount of slip required during an earthquake (or more generally during a period of strain release) to totally release the strain that accumulated during that period [Scholz and Fitch, 1969]. There is a reversal in sense between the virtual and real slip consistent with elastic rebound theory as illustrated in Figure 1. The estimated amount of virtual (reversed) slip for the entire pre-seismic period of 92 years between the last two Nankaido earthquakes in 1854 and 1946 is shown to be nearly equal to the net amount of forward slip for the seismic and post-seismic period from 1947 to 1950. Thus computed slip (either real or virtual) for the pre-seismic as well as seismic and post-seismic stages of the earthquake sequence provides simple quantitative support for an elastic rebound mechanism for underthrusting in southwest Japan.

Profiles of vertical displacement in regions A, B, C, and Kii (Figure 3) for ~~the three~~ each stage~~s~~ of the earthquake sequence are shown in Figures 12, 13, 14 and 15. It is convenient to divide the focal region into sub-regions small enough so that within each sub-region the displacement field is nearly one dimensional. Solutions to these one dimensional fields (Table III) can be computed from simple models in which the fault surface is rectangular and slip is uniform. The solutions are further simplified by restricting the fault models to those with the same trace and the same dip (35° northwest) as Model B. The remaining variables are the slip and down-dip length of the fault. Values for these variables as well as standard deviations between measured and theoretical displacements are tabulated in Table III.

There is a systematic misfit between the measured and computed profiles of seismic movements in regions A, B and C (Figures 12, 13, and 14). The computed profiles have gradients that are consistently too small near the region of maximum subsidence. Apparently fault models restricted to uniform slip on a rectangular surface are too simple. A few computations with models that include a gradient in slip in the down-dip direction suggest that such models are sufficiently general to account for the larger gradients in the measured profiles. Evidence from post-seismic movements discussed in a separate sub-section is also suggestive of non-uniform slip in the down-dip direction. Alternatively deviations from a planar fault surface may explain all or part of the misfit between the measured and computed profiles. In any case the size of the misfit is not large enough to necessitate a revision in the fault models.

To gain some insight into the error that results from extrapolating the solution for a particular sub-region to the focal region as a whole consider solutions to the displacement field that was generated at the time of the earthquake. The solutions (Table III) for the profiles Kii and C account for the greater deformation toward the western end of the focal region by an increase in slip from 6 to 18 meters and an increase in length of the fault from 55 to 90 km. Comparing these values of slip and down-dip length with those in Model B (Figure 8) shows that the solutions for the sub-regions overestimate the value of these variables in the eastern part of the focal region and underestimate them in the western part. For the slip the discrepancy is approximately a factor of 2. For the down-dip length the discrepancy is less than 25%. In the remainder of this section computed values of the fault parameters correspond to solutions to movements in a given sub-region for a given stage of the earthquake sequence.

Pre-Seismic Movements. Extensive leveling surveys [Geogr. Surv. Inst. of Japan, 1967] show that the reversal in sense between seismic and pre-seismic movements was a regional phenomenon. From this evidence it is concluded that strain build-up throughout the focal region accounts for these movements. A reversal in the direction of tilting at Muroto Point has already been discussed. A similar reversal in tilt occurred at the tip of the Kii peninsula [Okada, 1960]. In addition a rise in sea-level at the tip of the Kii peninsula, for at least a 28 year period, before the earthquake [Imamura, 1928] was reversed after the earthquake [Okada, 1960].

The initial leveling survey of Shikoku was completed in 1895. Part of the network that follows the southern coast was surveyed in 1929. A survey line that crosses the western end of the island (Region C in Figure 3) was resurveyed in 1938. For the Kii peninsula the initial survey followed the coast and was completed between 1886 and 1907. The second survey was completed in 1928. Results of the pre-1930 surveys are summarized by Tsuboi [1933]. In addition the western side of the southeastern peninsula of Shikoku was surveyed a third time in 1935 [Okada and Nagata, 1953].

The absolute datum for pre-seismic surveys on Shikoku and the Kii peninsula [Imamura, 1929 and 1930] was determined from secular changes in local mean-sea-level at the tide stations Komatusima (midway along the eastern coast of Shikoku) and Kusimoto (at the southern tip of the Kii peninsula). In general secular changes in sea level are difficult to determine because pressure and temperature variations [Yamaguti, 1968a] and drift of offshore currents [Hayashi, 1970] as well as ~~the~~ tidal components mask secular trends that may be present. However, in southwest Japan and presumably in other regions of active tectonism earthquake related movements are large enough to establish secular trends from mean-sea-levels for 10 to 20 year periods

[Yamaguti, 1968b]. Yearly mean-sea-levels at Kusimoto [Imamura, 1928] for the period from 1899 to 1927 show that sea-level was rising (or the land was subsiding) at a rate of nearly 1/2 cm/yr. The data from Komatusima is not as convincing, however. Within an uncertainty of a few centimeters, which may be an overly conservative estimate, ~~the~~ local mean-sea-level at this station did not change during the period from 1895 to 1928 [Imamura, 1930].

Pre-Seismic and Seismic Movements. From a comparison between the pre-seismic and seismic profiles ~~shown in Figures 12, 14, and 15~~, it is apparent that to a first approximation a reversal in the sense of motion occurred throughout the focal region. However, the reversal was not perfect, as Miyabe [1955] pointed out. Consider as guides the hinge lines represented in Figures 12, 14 and 15 by inflextion points between subsided and uplifted regions. The position of the hinge line for the permanent deformation in southeastern Shikoku is known within an uncertainty of a few kilometers (in a direction perpendicular to the inferred strike of the megathrust) from careful mapping of different sets of uplifted terraces [see e.g. Watanabe, 1948; and Yoshikawa et al., 1964]. Similarly the position of the hinge line for the permanent deformation of the Kii peninsula is uncertain by approximately the same amount [Yonekura, 1968]. The uncertainty in the hinge lines for the pre-seismic movements of eastern Shikoku and ~~the~~ western Kii peninsula depends strongly on the absolute datum (in this case a change in mean-sea-level) for each region during the pre-seismic period. As is evident from Figures 12 and 15 an error of a few centimeters in the absolute datum, which is a reasonable estimate for Shikoku, however probably an overestimate for the Kii peninsula, would cause a 10 km shift in the hinge line in each region. By a similar argument the hinge lines for the seismic movements are uncertain by approximately the same amount based on the previously discussed uncertainty of about 10 cm in the absolute datum for these movements ~~at the time of the earthquake.~~

As shown in Figure 15 the hinge lines for the permanent deformation and the pre-seismic movements in the western Kii peninsula are in the same position within the probable errors mentioned above; however, the hinge line for the seismic movement is a significant distance farther south (about 35 km). Similarly Figure 12 shows that the hinge line for the seismic movements in Region A is farther south than the hinge lines for the permanent deformation and the pre-seismic movements; however, the disparity is only 15 km and only marginally significant in view of the above mentioned uncertainties. Thus, with some caution, one may conclude that the permanent deformation given by the terraces and the pre-seismic movements are more nearly the reverse of each other than are the pre-seismic and seismic movements.

Solutions to the pre-seismic profiles across regions A and Kii given in Table III show that the virtual slip, normalized to the recurrence time between successive Nankaido earthquakes, is less than half of the slip released at the time of the 1946 earthquake. In addition there is some indication from these solutions that the virtual slip accumulated on a surface that was longer (in the down-dip direction) than the fault surface that ruptured at the time of the earthquake.

A comparison between pre-seismic and seismic movements in Region C near the western end of the focal region reveals an apparently exact reversal in sense; however, movements near the hinge line that showed a disparity in this reversal in Regions A and Kii occurred on the continental slope and thus are unknown. The profile of pre-seismic movements in Region C not only shows that the entire region was uplifted but that this uplift was greater than pre-seismic uplifts in regions A and Kii. This observation is suggestive of greater strain accumulations near the western end of the fault surface and correspondingly greater slip at the time of the earthquake as shown by the previously described fault models A and B and by the solutions to the seismic movements given in Table III. The computed solutions to the pre-seismic movements given in this table show that virtual slip is at least four times greater on the fault surface beneath Region C than on fault surfaces beneath regions A and Kii. Thus the magnitudes as well as the sense of the virtual dislocations computed from pre-seismic movements support a model for strain build-up consistent with rebound theory.

Post-Seismic Movements. The regional extent of the post-seismic movements was clearly revealed by reobservation of the leveling network in western and southeastern Shikoku. Post-seismic movements in Figure 14, from surveys of western Shikoku completed in 1948, 1950 and 1964, show that elevation changes in Region C near the western end of this rupture extended across the entire width of the island. Surveys completed in 1947 and 1964 of the network in southeastern Shikoku revealed post-seismic movements in Region A (shown in Figure 12) that were locally of the same magnitude as movements at the time of the earthquake. Post-seismic movements similar to those in Region A can be inferred from tilting and changes in mean-sea-level near the tip of the Kii peninsula [Okada, 1960]. Post-seismic movements of large magnitude were also recorded as changes in local mean-sea-level at 4 tide stations operated at widely separated locations along the coast of Shikoku. These data are shown within insets in Figure 5.

In general, changes in sea-level at these stations during the recovery period occurred at rates more than one order of magnitude larger than the pre-earthquake rates reported by Imamura [1928 and 1930]. In south central Shikoku at tide station Urado sea level rose by approximately 800 mm at the time of the earthquake followed by a drop of almost 300 mm at a rapidly decaying rate during the period from 1947 to 1950. Between 1950 and 1967 mean-sea-level at Urado corrected for temperature and pressure variations [Yamaguti, 1968a] fell an additional 100 mm ± 25 mm. At Uwazima on the western coast of Shikoku sea-level rose by 290 mm at the time of the earthquake. Following the earthquake sea-level rose 110 mm in a three year period. Simizu, near Ashizuri point (the tip of the southwestern peninsula of Shikoku), recorded a drop in sea-level of approximately 400 mm at the time of the earthquake. In the three year period following the earthquake, sea-level at Simizu rose 60 mm. The rise in sea-level at these latter two stations during the recovery period is difficult to interpret because both stations are near the western end of the rupture and thus movements at these stations are influenced by any peculiarities that may have occurred at the end of the megathrust. On the northeastern coast of Shikoku, station Takamatu recorded a small rise in sea-level at the time of the earthquake followed by a three year period in which sea-level rose 270 mm. The usefulness of data from Takamatu is somewhat diminished because the network of level lines used in the pre-seismic and the first post-seismic survey was not completely resurveyed in 1964 at the time of the most recent survey.

Changes in sea-level at Takamatsu are consistent with a general subsidence at the time of the earthquake that occurred in a broad region inland from the peninsulas and showed that continued subsidence occurred at a decreasing rate during the recovery period. Thus the seismic and post-seismic movements had the same sense in the vicinity of Takamatsu. In contrast data from tide station Urado adjacent to the uplifted south eastern peninsula of Shikoku showed a reversal in sense between seismic and post-seismic movements. An adjustment by slip on the fault surface that ruptured during the earthquake such that slip on lower and upper portions of the fault are reversed in sense during the recovery period can at least qualitatively explain the seismic and post-seismic movements ~~inferred from changes in sea-level~~ at these two tide stations. This idea will be pursued quantitatively. ~~in the following subsections.~~

Post-Seismic and Seismic Movements. The post-earthquake data from the eastern part of the focal region were surveyed mainly in Region A. These data as well as other post-seismic data from Shikoku were tied to a smoothed record of mean-sea-level at tide station Urado. This profile (Figure 12) shows that region A underwent a net uplift between 1947 and 1964. Uplift reached a maximum of nearly 600 mm at the center of the local depression that occurred in the zone of subsidence at the time of the earthquake. Note that the seismic and post-seismic profiles show that tilt of the southeastern peninsula of Shikoku in the vicinity of Muroto Point was reversed following the earthquake as previously discussed, even though the uplift of the peninsula continued.

The sum of the seismic and post-seismic profiles for Region A looks like the reverse of the pre-seismic profile (Figure 12); however, the hinge line for these movements is north of the hinge line for the terraces. At least part of this discrepancy is due to an almost unavoidable error in the surveying technique. Following the main shock it took nearly one year to complete the initial post-earthquake survey. Most of the recovery movements ~~interpreted as adjustments in slip~~ took place during this period. The resulting error in the post-earthquake data from Region A, although difficult to measure quantitatively is in the correct sense to move the hinge line too far to the north. Apparently the pre-seismic and seismic movements are not exactly the reverse of one another as simple rebound theory would predict but the pre-seismic and the sum of the seismic and post-seismic movements are the reverse of one another. This result constitutes an important modification to simple rebound theory.

The shape of the post-seismic profile for Region A is suggestive of slip on a buried fault (Figure 12); however, an acceptable solution to this displacement field assuming uniform slip on a buried fault was impossible. By comparing the solution to the sum of the seismic and post-seismic profiles with the solution to the seismic profile (Table III) it was possible to infer ~~deduce~~ the following post-seismic movements: approximately 5 meters of forward slip (or creep) on a 30 km extension of the fault down dip and reversed slip of 2 to 3 meters on that part of the fault that ruptured at the time of the earthquake. These results have been corrected for virtual slip equivalent to strain accumulation in the periods from 1929 to 1947 and from 1950 to 1964.

Although post-earthquake data from the Kii peninsula are much less conclusive than the data from Region A, there is evidence from tilts and changes in sea-level [Okada, 1960] for movements similar to the post-earthquake movements in Region A; i. e., post-seismic uplift near the tip of the peninsula was probably more pervasive than uplift at the time of the earthquake. In fact post-earthquake uplift in southern Kii would have to be more pervasive than similar movements in Region A (the adjacent coast of Shikoku), to bring the hinge lines for the sum of the seismic and post-seismic movements into coincidence with the hinge lines for the terraces and pre-seismic movements.

From solutions to the displacement fields in Regions A and Kii it is apparent that the sum of pre-seismic virtual slip (normalized to a 100 year period), seismic slip and post-seismic reversed slip (same sense as virtual slip) is nearly zero. This is another way of stating the generalized version of rebound theory. By a simple yet appealing analogy with oscillating systems the reversal in slip can be thought of as overdamped recovery to underdamped motion on the fault surface at the time of the earthquake. Such damping could be explained by ordinary Coulomb friction as well as by viscoelastic dissipation. The decay curves describing post-seismic changes in sea-level at Urado (Figure 5) as well as tilting near Muroto Point and the southern tip of the Kii peninsula are suggestive of a transient mechanism such as the proposed mechanism of overdamped recovery. In a similar manner inferred forward creep along the base of the megathrust suggests that part of the motion on this part of the fault at the time of the earthquake was overdamped, or that the fault extended itself into previously unslipped regions.

These conclusions are further strengthened by evidence from that portion of the western end of the focal region in Region C. Post-seismic movements uplifted the southern part of this region during a two year period and caused subsidence in the northern part. This subsidence is consistent with independent evidence (previously discussed) ~~of~~ For a rise in sea level during this period at tide station Takamatu located on the northeastern coast of Shikoku. A computed solution to this profile using all the data points has a standard deviation of nearly 1/2 the value of the largest displacement in the profile (Table III). If the data points showing subsidence are eliminated from the calculation a solution to the remaining profile is consistent with reversed slip or back sliding of nearly five meters on a fault surface with a down-dip length of 70 km. This solution overestimates the reversed slip and underestimates the length of the fault. Such a bias is caused by restricting the class of models to those with uniform slip. With this restriction the sign of the slip is determined by movements on the shallower portion of the fault surface because these movements in general cause the greatest surface displacements.

Alternatively, a solution was found for the sum of the seismic displacements as was done for displacements in Region A. From a comparison with this solution and the one for the movements at the time of the earthquake the following post-seismic slip is inferred: approximately three meters of reversed slip on that portion of the fault that ruptured during the earthquake and forward slip on a short down-dip extension of that fault surface. In any case the generalized version of rebound theory appears to apply to western as well as eastern portions of the focal region.

Post-recovery movements. The profile for the period 1950-1964 (Figure 14) is similar to the one for the period from 1948-1950 except that the zone of subsidence is less extensive. Solutions to this profile yield 6 to 7 meters of reversed and/or virtual slip on a fault surface that is approximately 3/4 as long as the fault that ruptured during the earthquake. Only one third of this slip can be accounted for by strain accumulation (judging from pre-seismic strain rate). Subsidence in the northern part of the region suggests that strain accumulation is competing with another process such as forward creep near the base of the fault. As a result solutions using fault models with uniform slip are biased as previously discussed. From this solution it is clear that the rates of deformation were reduced by more than a factor of seven from 1950 to 1964 in comparison with rates between 1948 and 1950. It is also possible that the inferred forward creep near the base of the fault continued after the three year period of rapid recovery; although there is no independent evidence such as a record of mean-sea-l evel at a local tide station to support this conclusion.

Mechanism of Underthrusting. The post-seismic movements triggered by the 1946 Nankaido earthquake are suggestive of a complex response to movements that occurred during the mainshock. The inferred back-sliding at a rapidly decaying rate on shallow portions of the megathrust is explained as a response to underdamped motion at the time of the earthquake. Consequently an over-shoot consistent with a stress drop of more than 100% occurred at the time of the main shock. Delayed forward creep on down-dip extensions of the fault can be interpreted as a response to overdamped motion near the base of the fault during the earthquake. These results are strongly in conflict with the traditional concept of faulting as a critically damped process. Thus the net slip during a period of strain release is in general the sum of slip during the mainshock and delayed slip (in the forward and/or reversed sense) during a period of post-seismic adjustment.

In approximately the western 1/3 of the focal region where the inferred over-shoot at the time of the earthquake was most extensive there was no aftershock activity. Thus, as in the case of the Parkfield earthquake, the recovery movements had no seismic expression. In the remaining 2/3 of the focal region where the down-dip extension of the fault by delayed forward creep was most extensive, the aftershock zone also extended itself in the same direction; i.e., toward the north [Mogi, 1968]. This correlation between forward creep and aftershock activity is consistent with results from numerous aftershock studies showing that the mechanism solution for most aftershocks are similar to ~~the mechanism of~~ that for the mainshock [e.g., see Stauder and Bollinger, 1966b; Stauder, 1968a].

PERMANENT DEFORMATION AND EVOLUTION OF TERRACES

The inferred mechanism of underthrusting for the 1946 Nankaido earthquake is consistent with a generalized version of elastic rebound theory; however, there is evidence for permanent deformation along the shorelines in the focal region of this and other recent megathrusts that is not predicted by rebound theory. A correlation between the spatial distribution of uplift at the time of a major earthquake and the distribution of permanent uplift within the focal region similar to that established for the Kanto region of Japan [Sugimura and Naruse, 1954 and 1955] was also established for the focal region of the Nankaido earthquake [Yoshikawa, 1970]. Several sets of uplifted marine terraces are mapped near the shorelines of three peninsulas (Figure 3) within the focal region of the 1946 earthquake [Watanabe, 1932; Yoshikawa et al., 1964; Yonekura, 1968]. Careful observation of the terraces in south-eastern Shikoku showed that steps between major terraces often include one or more small steps suggestive of intermittent uplifts associated with major earthquakes such as the one in 1946 [Watanabe, 1932]. Similar geomorphological evidence coupled with known vertical movements at the times of the last two Nankaido earthquakes show that marine terraces along the southern coast of the Kii peninsula were formed in the same manner as those in eastern Shikoku [Yonekura, 1968].

The assumptions required to quantitatively estimate the rate of permanent tilt from available geodetic data were already discussed with reference to data from the vicinity of Muroto point. Similar assumptions can be used to estimate the rate of permanent deformation for the entire southeastern peninsula including Muroto point. A quantitative outline of this argument is given in Table IV. The estimated permanent tilt or net tilt of this peninsula resulting from the latest earthquake sequence is 2.7 sec which is in reasonable agreement with tilt rates of about 1 sec/century inferred from the present tilts and ages of two of the older terraces. Note that the measured tilts unlike heights are independent of eustatic changes in sea level.

Of three recognizable sets of terraces, an age of 6000 years for the youngest set was determined radiometrically in the Kanto region of south-central Honshu [Yoshikawa, 1970]. This age corresponds to the most recent sea-level maximum in Japan [Yoshikawa et al., 1964]. By analogy the ages of the older terraces are thought to correspond to world-wide maxima in sea-level during two previous interglacial stages [Yoshikawa et al., 1964]. By this dating method the oldest set of terraces, called the Hane-saki terraces, is about 170,000 years old. However, aside from present sea-level that apparently has remained nearly constant for the last few thousand years [Curray et al., 1970] time correlations between local sea-level maxima in different regions have revealed only one generally recognized world-wide maximum, the one that occurred approximately 120,000 years ago [see e.g., Broecker et al., 1968]. Thus the estimated ages of the older terraces must be considered as tentative until they are dated radiometrically.

On the eastern side of the southwestern peninsula of Shikoku near Ashizuri point is another set of uplifted terraces [Watanabe, 1948]. These terraces are not as well developed as the ones near Muroto. In fact the eastern side of this peninsula subsided at the time of at least one major earthquake, the one in 1707. At the times of the 1854 and 1946 earthquakes this coast was uplifted [Watanabe, 1948]. Since this peninsula is near the western end of the megathrust that ruptured in 1946 and presumably is also near the end of previous ruptures, it seems reasonable to explain uplift or subsidence of this peninsula during past earthquakes by small changes in the westward extension of the rupture.

In southwest Japan as well as other regions of underthrusting the uplifted terraces in a crude sense provide a record of underthrusting for periods of time as long as tens of thousands of years. The age, spatial distribution and the present tilt of terraces in southwest Japan is in reasonable agreement with the rate and regional extent of permanent deformation inferred for the Nankaido earthquake sequence from 1854 to 1946. If the ages of the terraces and eustatic sea-level changes were known with greater accuracy heights of the terraces as well as tilts could be used to compute average rates of underthrusting for periods of tens of thousands of years. Such a method may provide a more stable measure of recent underthrusting than that computed by the method of seismic moments [Brune, 1968].

TECTONIC IMPLICATIONS

Introduction. The estimated age of the oldest terraces in southwest Japan provides a minimum estimate for the onset of underthrusting in this region of approximately 100,000 years ago. This portion of Japan between the Ryukyu and the junction of the Honshu and Izu-Bonin arcs (represented in Figure 2 by the Japan, Ryukyu, and Izu-Bonin trenches) has been tectonically stable by comparison with the adjacent well-developed island arcs that have been active since the late Cenozoic [see e.g., Minato et al., 1965; Matsuda et al., 1967; Huzita, 1969; Sugimura and

Uyeda, 1970]. Moreover, folding [Huzita, 1969] and fault movements [Huzita, 1969; Allen et al., 1970] since the early Pleistocene as well as numerous mechanism solutions for shallow earthquakes [Ichikawa, 1965] suggest that interior portions of southwest Japan including portions of the focal region for the 1946 Nankaido earthquake, have been and still are deforming in response to a regional east-west compression; rather than a southeast-northwest compression consistent with the inferred direction of underthrusting normal to the Nankai trough.

An east-west trend in regional compression is nearly perpendicular to the Honshu arc which judging from recent seismicity [see e.g., Gutenberg and Richter, 1954], is the most active of the island arcs adjacent to southwest Japan. In terms of plate tectonics regional stress in central and western Japan appears to be dominated by a compression generated by the convergence of the Asian and Pacific Ocean plates along the deep-sea trench adjacent to the Honshu arc. This conclusion is consistent with estimates of rates of convergence for this region (to be presented later) showing that the Asian and Pacific plates are converging at a higher rate than the Philippine Sea and Asian plates or the Pacific and Philippine Sea plates.

The inner "craton-like" portion of southwest Japan is separated from a series of Paleozoic to mid-Tertiary formations to the south by a narrow metamorphic zone of Mesozoic age [Huzita, 1969]. The median tectonic line (Figure 2) within this metamorphic zone marks the boundary between two paired metamorphic belts [Miyashiro, 1967] that are thought to be relics of two Mesozoic island arcs [Matsuda et al., 1967; Dewey and Bird, 1970]. Kaneko [19~~69~~66b] and Allen et al. [1970] recently have presented evidence for Pleistocene to Recent movements in the right lateral sense on faultlike features paralleling the median line. Profiles of vertical displacement in Shikoku and the Kii peninsula shown in Figures 12, 13, 14, and 15 are not offset at points where the survey network crosses the median line. Thus the possibility of a causative relationship between movements in the zone of underthrusting along the Nankai trough and those along the median line can not be established. However, continued underthrusting of the Philippine Sea plate beneath southwest Japan should eventually (depending on the slip rate) have a more obvious surface expression consistent with the development of structures typical of island arcs such as active volcanoes and a well-developed deep-sea trench.

Slip Rate in Southwest Japan. A slip rate between the Philippine Sea and Asian plates in the region of the Nankai trough can be estimated from the computed slip during the 1946 Nankaido earthquake and the average recurrence time of such events. The preferred fault model (Model A illustrated in Figure 8) indicates that slip for the 1946 earthquake varied from 5 meters in the northeast to 18 meters in the southwest. If such a gradient in the slip was stable over long periods of time the center of rotation for the Philippine Sea and Asian plates would be very near southwest Japan. Since stability of the slip gradient cannot be established, the average slip of 12 meters is considered the most reliable measure of underthrusting during this earthquake. Consideration of the backsliding after the earthquake as a response to overshoot leads to a reduction of the average slip to 8 ± 4 meters, which for the recurrence interval of 100 years yields a slip rate of 8 ± 4 cm/yr. Although slip is one of the least well-determined parameters of the fault models, the accuracy of this slip rate is probably comparable with the accuracy of seismic slip rates [Davies and Brune, 1971] or those determined from magnetic anomalies [e.g., see Le Pichon, 1968] computed for other regions. If the age of the oldest set of terraces (the Hane-saki terraces) is accepted as 170,000 years then the Philippine Sea plate has been descending beneath southwest Japan at nearly this rate for at least that period of time.

If underthrusting adjacent to the Nankai trough has continued at this rate for one million years the length of the inclined slab would be 80 km and the bottom of the slab would be nearly 50 km beneath the bottom of the lithosphere or nearly 100 km beneath the surface. This is probably an overestimate of the depth to the deepest earthquakes in this part of Japan based on accurate hypocenter determinations [e.g., see Ichikawa, 1961 and 1965; Minato et al., 1965]. The absence of active volcanism in this part of Japan suggests that the slab has not reached depths greatly in excess of 100 km because volcanoes in adjacent parts of Japan form above those parts of the inclined seismic zones in the depth range between 100 km and 200 km [e. g., see Matsuda et al., 1967]. This evidence favors a geologically recent onset of underthrusting along the Nankai trough. An onset less than one million years ago may be reasonable.

There is also evidence from echograms across the Nankai trough consistent with a geologically recent onset of underthrusting [Hilde et al., 1969]. The turbidites in the trough appear to have the same distribution as those in the adjacent basin except for the topmost layer that thins toward the outer wall of the trough. Hilde et al. [1969] suggested that this layer formed since the trough began subsiding after the onset of underthrusting. If this is true then the thinness of the layer suggests that underthrusting started in geologically recent time. Similar evidence cited by Heezen and Laughton [1963] and Hamilton [1967] shows that the formation of the Aleutian trench adjacent to south-central Alaska cut off the supply of sediments that was accumulating on the adjacent abyssal plain.

Slip in the Northern Izu-Bonin Region. A triple point is formed by the intersection of the Japanese and Izu-Bonin trenches and the Nankai trough [McKenzie and Morgan, 1969]. If the lithosphere in this region can be approximated by rigid plates, one of the three slip vectors describing relative convergence between the plates in the vicinity of the triple point is completely determined by the other two. The slip vector computed above for recent convergence of the Philippine Sea and Asian plates in southwest Japan has a trend normal to the Nankai trough and a magnitude of 8cm/yr. The direction of slip between the Asian and Pacific plates in this region inferred from slip vectors determined from magnetic anomalies [e.g., see Le Pichon, 1968] and mechanism solutions for recent earthquakes [Isacks et al., 1968] is nearly perpendicular to the Japanese trench. For an estimate of the rate of convergence along the Japanese trench the seismic slip rate of 22cm/yr [Davies and Brune, 1971] was chosen ~~arbitrarily~~ because it is consistent with the rate of 8cm/yr inferred for southwest Japan in that southwest Japan ~~is~~ has been seismically much less active ~~at present~~ in recent years than the region of the Japanese trench. Rates of convergence determined from magnetic anomalies [e.g., see Le Pichon, 1968], are as much as a factor of two less than the seismic rate.

The seismic rate of 22cm/yr may be an overestimate. If overshoot similar to that inferred for the 1946 Nankaido earthquake also occurred during underthrusting on the continental slope adjacent to the Japanese trench the computed seismic slip would be overestimated. A similar bias of nearly 10% would result if the 1933 Sanriku earthquake was included in this estimate because, as Kanamori [1970] showed, this event occurred on a normal fault and thus did not contribute to convergence between the plates. If this is a region of high stress as Mogi [1968] suggested based on the comparatively small size of the aftershock zones, the seismic slip would again be overestimated. Although it is impossible to accurately estimate the error in this slip rate Davies and Brune [1971] suggest that in general estimates of seismic slip can be in error by a factor of two or more.

From computed rates and directions of convergence between the Asian and Pacific plates and the Asian and Philippine Sea plates in the vicinity of the triple point it is easily shown (Figure 16) that the Pacific and Philippine Sea plates are converging along a strike nearly normal to the Izu-Bonin trench and at a rate of nearly 17 cm/yr. A large slip rate such as this is consistent with the length of the deep seismic zone beneath this arc. Prior to this study slip vectors between the Philippine Sea and Pacific plates were unknown due to the absence of a simple spreading ridge in the Philippine Sea and a lack of recent shallow earthquakes of large magnitude along the convex side of the Izu-Bonin Arc [Le Pichon, 1968; Katsumata and Sykes, 1969].

A slip rate for this arc inferred from moments of shallow earthquakes [Davies and Brune, 197~~0~~1] is approximately one order of magnitude less than that computed from the plate model used in this study. This disparity can be explained by a temporary decrease in seismic activity; however there may also be a fundamental error in the assumed plate model for this region. E.g. Karig [1971] suggested that a series of en echelon troughs within the northern Izu-Bonin arc may be the beginning of an inter-arc basin such as the one west of the Mariana arc. If this is correct the rigid plate assumption must be modified and consequently at least part of the slip between the Asian and Philippine Sea plates may result from spreading within the plate.

Stability of the Triple Point. The intersection of three trenches poses a stability problem [McKenzie and Morgan, 1969]. In general a triple point formed by three trenches is unstable; i.e., it will move relative to whichever plate contains the coordinate system. Because the slip vectors between the three plates are nearly perpendicular to their respective trenches the stability criterion is trivial: the triple point is stable only if two of the trenches are perpendicular to each other. The strike of the Nankai trough is within 11° of being perpendicular to the Izu-Bonin trench. Therefore regardless of the magnitude of the slip vectors the triple point will move slowly if at all. If the seismic slip vectors discussed previously are assumed to be reasonable approximations to the long-term average vectors, then by the construction shown in Figure 16 the triple point migrates toward the south along the Nankai trough about 14 km in one half million years or 0.3 cm/yr. This migration rate is more than one order of magnitude less than that suggested by McKenzie and Morgan [1969]; however, in contrast to experimental evidence presented in this study, they assumed that the slip vector adjacent to southwest Japan was not perpendicular to the Nankai trough in which case much larger rates of migration are possible.

SUMMARY

The mechanism for the 1946 Nankaido as well as other megathrusts can be visualized as a spring loaded block in frictional contact with an inclined plane. In this simple system the ratio between the dynamic and static friction (that for a real fault in general is a function of time and position on the fault surface) will control the motion of the block. The maximum amount of stored elastic energy is determined by the static friction. If a continuous driving mechanism is provided such a system will respond by a sequence of movements that will be periodic as long as it is driven at a constant rate [e.g., see Burridge and Knopoff, 1967].

In terms of plate tectonics the idealized model previously described is analogous to a boundary between converging plates of lithosphere illustrated in Figure 17. The focal region for such a megathrust is hundreds of kilometers wide and thus includes most of the adjacent island arc. During pre-seismic periods the fault is "locked" and the leading edge of the megathrust is dragged down with the descending slab of lithosphere. Although the driving mechanism or mechanisms for this convergence as well as the remaining global pattern of plate movements are not completely understood these movements are undoubtedly driven at rates that are constant during periods of time that are long in comparison with recurrence times for major earthquakes. Thus a constant rate of strain buildup might be expected along those portions of the plate boundaries where earthquake sequences include relatively long periods when the boundary is locked.

When friction between the opposing plates of lithosphere can no longer keep the fault from slipping an episode of strain release is initiated, most of which occurs during a major earthquake. Net movements during periods of strain release, illustrated in the lower diagram of Figure 17, is opposite in sense to pre-seismic movements. Following a period of strain release that may last several years, as was the case for the 1946 Nankaido earthquake, a new period of strain buildup begins.

In regions of underthrusting one can imagine a sequence of movements consistent with rebound theory such that there is no permanent deformation of the free surface which with reference to the model in Figure 17 would imply that the overlying plate of lithosphere is dragged down from an equilibrium position before an earthquake and returns to that position after the earthquake. During such a sequence of movements the oceanic lithosphere would descend (in a down-dip direction) into the upper mantle a distance equal to the amount of slip between the plates. Contrary to the earthquake sequence just outlined, numerous examples of uplifted terraces in southwest Japan and in several other regions of underthrusting are conclusive evidence for permanent deformation that is a common and possibly inevitable consequence of underthrusting.

A possible explanation for this permanent deformation is that the overlying plate of lithosphere overrides the oceanic lithosphere at the time of underthrusting, thereby causing a flexure in the overriding plate that along portions of the shoreline is recognized as a low terrace. This explanation implies that there is a regional compression driving the plates of the lithosphere together. As illustrated in Figure 17, a flexure caused by overriding will grow with each episode of strain release and thus impose increasing stress on the converging plates unless such stress is relieved by faulting or some other form of stress relaxation.

In Japan and other regions of plate convergence there is a spatial correlation between permanent uplift or subsidence of shorelines and the displacement fields generated by major underthrusting. Such a correlation is suggestive of a permanent flexure in the overriding plate that results from successive underthrusting movements. Vertical movements within the focal regions of the last three Nankaido earthquakes correspond closely to the distribution of permanent uplift or subsidence of shorelines; i.e., peninsulas nearest the epicenters are uplifted and a broad zone of subsidence is formed behind the peninsulas. In southwest Japan these movements have continued for approximately 100,000 years and possibly much longer depending on the time for the onset of underthrusting. Along the east coast and other parts of the southwest coast of Honshu there is evidence for a similar correlation between peninsulas with permanently elevated shorelines and intermittent uplift during large off-shore earthquakes [e.g., see Watanabe, 1959]. Similar evidence, although based on fewer and less precise observations, have been reported from other zones of underthrusting; e.g., in south-central Alaska [Plafker and Rubin, 1967; Plafker, 1969] and in Chile [Plafker and Savage, 1970].

Indirect evidence suggests that near focal regions of some recent megathrusts there is a change in tectonic stress consistent with the evolution of flexures similar to those illustrated in Figure 17. Sykes (personal communication) pointed out an apparent time correlation between earthquakes with extensional mechanisms consistent with normal faulting on the outer walls of deep-sea trenches and recent underthrusting on adjacent portions of the inner walls of these trenches. For example, Isacks [1970] found that after the Chilean megathrust there was normal faulting in the sediment-filled trench adjacent to the aftershock zone during the period from 1963 to 1965. The onset of this activity is not known because data were lacking for the two years immediately following the series of mainshocks in May of 1960. Stauder [1968b] reported several solutions of this type for earthquakes in the Aleutian trench. Although this activity does not correlate perfectly with recent underthrusting this trench does parallel one of the most active zones of recent underthrusting. In contrast there has been in recent years little evidence for normal faulting from recent earthquakes with $M \geqq 6$ in the Tonga-Kermadec trench (Molnar, personal communication); neither has there been a major episode of underthrusting adjacent to this trench [Isacks et al., 1969]. Thus there appears to be a correlation (the details of which are not understood) between major underthrusting on the inner walls of deep-sea trenches and extension on the outer walls that may be explained by flexural strain generated by overriding of the underthrust plate.

Sequences of movements similar to that illustrated in Figure 17 are undoubtedly in progress on most if not all boundaries between converging plates of lithosphere. In general these earthquake sequences are not completely in phase with one another as evidenced by the fact that earthquakes rupturing the plate boundaries do not occur at the same time. For example, in southwest Japan the release of accumulated strain along most of the plate boundary between the Honshu and Ryukyu arcs occurs by either a short series of large earthquakes closely spaced in time such as occurred in the mid-1940's and in 1854 or by a single great event such as occurred in 1707 [Imamura, 1928].

In regions of island arc tectonics such as Japan the great thrust faults on the convex sides of the arcs generate vertical and horizontal movements that can be measured by geodetic methods across the entire width of the islands (e.g., see Figures 9 and 10). Measurements within a given focal region during pre-seismic periods will reveal movements that are opposite in sense and much smaller in magnitude than seismic movements. The sum of movements during repeated geodetic surveys throughout the island arc will in general include seismic and pre-seismic movements generated at different times along different segments of the thrust zone. The sum of these out of phase movements cannot be interpreted as permanent deformation of the island arc because 80 or 90% of this sum is eventually recovered during earthquakes and post-earthquake adjustments.

For the 1946 Nankaido earthquake movements during each of the three stages in the earthquake sequence, the pre-seismic, the seismic, and the post-seismic stage, are interpreted as slip, either real or virtual (strain buildup), on the surface of a complex megathrust. In contrast to average parameters for the fault determined from seismic data the geodetic data reveal "fine structure" such as a gradient in slip parallel to the strike of the thrust. The post-seismic movements are shown to have a "memory" for the mechanism of faulting at the time of the earthquake; e.g., fault motion during the 1946 Nankaido earthquake inferred from post-seismic movements was underdamped on the upper portions of the fault surface and overdamped on the lower portions.

A potentially important implication of underdamped faulting is that the resulting over-shoot, unless recovered immediately will cause an overestimate of net slip between the plates. Inferred over-shoots at the time of the 1946 Nankaido earthquake account for 1/3 to 1/2 of the total slip in the forward direction. However, corrections of this magnitude at present are not important when estimating slip from seismic moments [Brune, 1968; Davies and Brune, 1971] because such estimates may be uncertain by a factor of 2 or more.

Problems encountered in interpreting faulting in terms of average plate motion can be avoided if as in the case of the 1946 earthquake the rate of virtual slip during periods of strain buildup is equivalent in magnitude to the average slip rate between plates. Thus repeated surveys during periods of strain buildup can be directly interpreted as relative plate motion. However, at least three surveys are needed during periods between major earthquakes to be certain that the movements are increasing at a constant rate. Nonlinear rates, if they exist, could suggest premonatory movements of a future earthquake or long-term adjustment from a past earthquake.

The 1946 Nankaido earthquake initiated a period of strain release that continued for approximately three years and included fault movements that were aseismic as well as seismic. The post-seismic deformation in the southwestern end of the focal region took place without aftershock activity whereas similar movements in the northeastern end of the focal region were accompanied by aftershock activity. This result is consistent with measurements of post-seismic movements (shown in Figures 12, 13, 14, and 15) showing that during the period of adjustment following the earthquake the rate of strain release in the northeastern part of the focal region was locally about five times greater than the rate in the southwestern part. Thus the size of the aftershock zone corresponds to areas within the focal region where strain is released at relatively high rates. The sum of these areas may not correspond to the total area of the rupture.

The rebound mechanism inferred for the 1946 Nankaido earthquake is clearly periodic in space as well as time. Additional geodetic data of high quality is needed to better understand the periodicity and thus the predictability of these and similar earthquakes. In the near future space-age methods for accurately measuring lengths over continental distances such as very-long-base interferometry (VLBI) and lasar ranging techniques will be available for obtaining these data [Williamstown Report, 1969].

For monitoring strain buildup in regions of underthrusting that are typically several hundred kilometers wide techniques such as those just mentioned are potentially far superior to standard geodimeter, triangulation and leveling methods because the problem of determining an absolute datum from which to compute displacements is eliminated when this datum can be fixed in a stable region thousands of kilometers from the zone of underthrusting. Frequent monitoring of strain buildup in regions where there are estimates of the total strain released during a major underthrust such as the regions of underthrusting in southwest Japan, south-central Alaska and Chile could provide essentially a continuous measure of earthquake risk. Because the largest of the world's earthquakes and tsunamis occur in regions of underthrusting, any technically feasible method for improving the predictability of these events should be developed as a matter of urgency. In addition, techniques for

C.2

accurately measuring lengths over continental distances can be used to confirm the theory of sea-floor spreading and continental drift by monitoring changes in distance between pairs of points in stable regions on opposite sides and at great distances from plate boundaries. The resulting drift rates could be used to more accurately predict future movements (at least in a gross sense) of the plates of lithosphere.

ACKNOWLEDGMENTS

Dr. Atusi Okada from the Earthquake Research Institute of Tokyo University sent us most of the geodetic data used in this study, including some unpublished data. He also provided copies of several articles referenced in the text, some of which were not available in this country. For his continuous interest and cooperation we are most grateful. Dr. K. Kanamori, also from the Earthquake Research Institute sent us a preliminary mechanism solution for the 1946 Nankaido earthquake based on the first motion of P waves. Dr. Mansinha gave us, prior to publication, compact equations for displacement fields generated by either dip-slip or strike-slip on an inclined dislocation in a half space. Throughout this investigation we benefitted from stimulating discussion with Prof. Lynn Sykes. Professors Sykes, Oliver and Isacks read the manuscript critically and suggested numerous improvements. This research was supported by a grant from the National Aeronautics and Space Administration.

FIGURE CAPTIONS

Figure 1 Elastic Rebound Models of Plate Boundaries.

A Transcurrent boundary: map view showing horizontal deformation, on a greatly exaggerated scale, of a line initially normal to the fault trace (dashed line) is shown by solid curves. The pre-seismic curve gives deformation of such a line during a period of strain accumulation, the seismic shows deformation by an earthquake, and the sum is the total deformation for the entire earthquake sequence. The heavy arrows give the long-term motion of one side of the fault with respect to the other side.

B Thrust boundary: vertical section; heavy arrows indicate long-term motion of one side of the fault with respect to the other side. Vertical deformation (on a greatly exaggerated vertical scale) of an initially undeformed free surface is shown by heavy solid curves. The fine lines in the three bottom figures mark the position of the initially undeformed surface.

Figure 2 Tectonic Setting of Japan and Adjacent Areas. Vertical and horizontal movements at the time of the Nankaido earthquake of 1946 occurred within the square. The dotted curve maps the trace of the Fossa Magna (the north striking line transverse to Japan) and the Median Tectonic Line [Richter, 1958]. Triangles represent terrestrial volcanoes that have been active historically and submarine volcanoes, of which some may not be presently active [Gutenberg and Richter, 1954].

Figure 3 Terraces and the Leveling Network in Southwest Japan. Along the coastlines of the striped regions are numerous examples of uplifted marine terraces [Watanabe, 193~~4~~2, 1948, 1959; Yonekura, 1968]. Leveling data used in this study comes from a network of survey lines mapped as dashed and dot-dashed curves [Geogr. Surv. Inst. of Japan, 1967]. Data for profiles A, B, C and Kii come from those parts of the network mapped as dashed curves. The large numbered dots correspond to principle bench marks. Epicenters of recent earthquakes of large magnitude are 1, the Nankaido earthquake of 1946, 2, the Tonankai earthquake of 1944, and 3, the Mikawa earthquake of 1945 with magnitudes of 8.2, 8.0 and 7.5 respectively [Matuzawa, 1964]. The checkered areas represent bathametric depressions, the most outstanding of which is the Nankai Trough [Kaneko, 1966a]. Areas T and H correspond to the Tosa and Hyuga basins respectively [Kaneko, 1966a].

Figure 4 The Recent History of Tilting at Muroto Point. This figure is adapted from a similar figure in Okada and Nagata [1953], and shows tilt of leveling lines projected on a vertical plane striking SSW near Muroto Point. NNE tilt is in the positive direction. A solid line or curve is used when the history of tilting is extrapolated between measured values. The length of the double headed arrow is an estimate of the permanent tilt at the time of the Nankaido earthquake of 1946.

Figure 5 Seismic Uplift and Subsidence of the Coastline. The dots give approximate locations for measurements (in centimeters) of uplift (positive) or subsidence (negative) at the time of the Nankaido earthquake [Geogr. Surv. Inst. of Japan, 1948; Watanabe, 1948 and 1959; Matuzawa, 1964]. The four insets are smoothed records from tide gauge stations originally presented in a report on the Nankaido earthquake edited by Kawasami in 1956 [Matuzawa, 1964]. Note tide gauge readings give changes in local sea-level thus a positive change in sea-level corresponds to subsidence of the coast.

Figure 6 Seismic Uplift and Subsidence of Southwest Japan. Contours of vertical displacement are based on data from leveling surveys of first order precision completed before and after the Nankaido earthquake of 1946 [Geogr. Surv. Inst. of Japan, 1967]. Contour spacing is 100 mm. Dots give locations of data points where contours cross the network of survey lines. Uplift relative to mean-sea-level is mapped by solid contours.

Figure 7 Seismic Activity and the Tsunami Generating Region. Recent earthquakes of large magnitude located in or near southwest Japan are identified by name and date [Matuzawa, 1964]. The arrows point to relocated epicenters for the Tonankai and Nankaido earthquakes. Relocated epicenters for aftershocks of the Nankaido earthquake reported in the ISS (International Seismic Summary) during the first month after the mainshock are identified by small solid circles (for the less well determined locations) and open circles (for better determined locations). The solid curves enclose the aftershock zone of the Nankaido earthquake and the southwest end of the aftershock zone of the Tonankai earthquake one month after the mainshocks [Mogi, 1968]. The most active zones of shallow earthquakes are mapped as striped regions [Imamura, 1928; Matuzawa, 1964; Ichikawa, 1965; Huzita, 1969]. The barbed line marks the surface trace of inferred thrust fault that ruptured at the time of the Nankaido earthquake. The heavy curve encloses the central source area for the tsunami generated by the Nankaido rupture [Hatori, 1966]. The Kinki triangle is a type area for late Cenozoic to Recent folding and faulting in the interior of SW Japan [Huzita, 1969].

Figure 8 Fault Models A and B. U, the slip, is given by the dashed lines. H, the down-dip length of the fault is given by the solid lines. Solid circles are projections of the epicenter for the main shock onto the inferred trace of the fault. The length and position of the aftershock zone one month after the mainshock are taken from Mogi [1968].

~~Figure 9~~ ~~Vertical Displacement Computed for Fault Model A.~~ Displacements are given in millimeters. Uplift is contoured with solid curves and subsidence is contoured with dashed curves. The closely spaced contours on the seaward side of the fault trace from north to south are 1 meter, 800 mm and 400 mm contours. Model A is illustrated in Figure 8 and discussed in the text.

Figure 10 Measured and Computed Horizontal Movements at the Time of the Nankaido Earthquake. Contours map the component of horizontal displacement (in meters) perpendicular to the strike of the fault computed for Model A (Figure 8); Solid contours ~~for~~ represent displacements in the southeasterly direction. The solid circles are locations of first order triangulation stations and the numbers are adjusted magnitudes of horizontal displacement in meters (see text for explanation). The heavy line between contours 1 and 1/2 represents the base line for the triangulation network.

Figure 11 Direction of Horizontal Movements. The solid arrows represent directions computed from triangulation data assuming a base line in central Honshu represented by the heavy line [Geogr. Surv. Inst. of Japan, 1952]. The dashed lines represent corresponding directions computed from Model A (Figure 8). The trace of the fault is represented by the barbed line.

Figure 12 Profile A. From top to bottom, pre-seismic, seismic, post-seismic and the sum of seismic and post-seismic vertical displacements (in mm) of eastern Shikoku (Region A in Figure 3) are projected onto vertical planes perpendicular to the inferred trace of the megathrust. The abscissa gives the distance (in km) from the trace of the megathrust. The dashed line represents the position of the hinge line for the marine terraces (Figure 2). The dotted curves are computed fits (in a least-squares sense) to the profiles (Table III gives the parameters for these solutions).

Figure 13 Profile B. Vertical displacements (in mm) of east-central Shikoku (Region B in Figure 3) during the Nankaido earthquake are projected onto a vertical plane perpendicular to the inferred trace of the megathrust. The abscissa gives the distance (in km) from the trace of the megathrust. The dotted curve is the computed fit (in a least-squares sense) to the profile (Table III gives the parameters for this solution).

Figure 14 Profiles C. From top to bottom, pre-seismic, seismic, first post-seismic and second post-seismic vertical displacements (in mm) of west-central Shikoku (Region C in Figure 3) are projected onto vertical planes perpendicular to the inferred trace of the megathrust. The abscissa gives the distance (in km) from the trace of the megathrust. The dotted curves are computed fits (in a least-squares sense) to the profiles (Table III gives the parameters for these solutions).

Figure 15 Profiles Kii. From top to bottom, pre-seismic and seismic vertical displacements (in mm) of the western coast of the Kii peninsula (Region Kii in Figure 3) are projected on vertical planes perpendicular to the inferred trace of the megathrust. The abscissa gives the distance (in km) from the trace of the megathrust. The dashed line represents the position of the hinge line for the marine terraces (Figure 2). The dotted curves are computed fits (in a least-squares sense) to the profiles (Table III gives the parameters for these solutions).

Figure 16 Slip and the Triple Point. The triangle illustrates the calculation of the slip vector (dashed line) for the Philippine Sea and Pacific plates knowing the slip vectors (solid lines) for the Asian and Philippine Sea plates and for the Asian and Pacific plates. Regions A, B, and C represent the Asian, Pacific and Philippine Sea plates respectively. The dashed outlines represent the configuration of the downgoing slabs after 1/2 million years of underthrusting. The migrations of the triple point (only 14 km) is given by the intersection (within the circle) of the dashed line representing the new position of the Izu-Bonin trench and the solid line representing the Nankai trough.

Figure 17 <u>Interaction Along a Convergent Plate Boundary.</u> In these schematic diagrams the shape of the free surface is greatly exaggerated near the boundary between the opposing plates. The arrows indicate the continuous descent of the oceanic lithosphere into the upper mantle. The "locking" of the plate boundary during pre-seismic strain buildup is graphically illustrated by the bolt holding the two plates together. At the time of an earthquake the bolt is sheared and slip occurs between the plates. Uplifted terraces are accounted for by the flexure in the overriding plate. Consequently a new equilibrium configuration for the plate boundary is established after completion of each episode of strain release. In the bottom figure the small opposing and oppositely directed arrows in the underthrust slab represent compression and tension respectively near the free surface.

REFERENCES

Allen, C.R., T. Matsuda and A. Okada, Relationship between seismicity and geologic structure in western Japan, Geol. Soc. Amer. (Abstract), p. 481, 1970.

Barazangi, M., and J. Dorman, World seismicity map of ESSA Coast and Geodetic Survey Epicenters Data for 1961-1967, Bull. Seismol. Soc. Amer., 59, 369-380, 1969.

Broecker, W.S., D.L. Thurber, J. Goddard, T. Ku, R.K. Matthews and K.J. Mesolella, Milankovich Hypothesis Supported by Precise Dating of Coral Reefs and Deep-Sea Sediments, Science, 159, 297-300, 1968.

Brune, J.N., Seismic moment, seismicity, and rate of slip along major fault zones, J. Geophys. Res., 73, 777-784, 1968.

Brune, J.N., and G.R. Engen, Excitation of mantle Love waves and deformation of mantle wave magnitude, Bull. Seismol. Soc. Amer., 59, 923-934, 1969.

Burridge, R., and L. Knopoff, Model and theoretical seismology, Bull. Seismol. Soc. Amer., 57, 341-372, 1967.

Chinnery, M.A., The deformation of the ground around surface faults, Bull. Seismol. Soc. Amer., 51, 355-372, 1961.

Curray, J.R., F.P. Shepard and H.H. Veeh, Late Quaternary sea-level studies in micronesia: Carmarsel expedition, Geol. Soc. Amer. Bull., 81, 1865-1880, 1970.

Davies, G.L., and J.N. Brune, Regional and global fault slip rates from seismicity, Nature Physical Science, 229, 101-107, 1971.

Dewey, J.F., and J.M. Bird, Mountain belts and the new global tectonics, J. Geophys. Res., 75, 2625-2647, 1970.

Fitch, T.J., Earthquake mechanisms and island arc tectonics in the

Indonesian-Philippine region, Bull. Seismol. Soc. Amer., 60, 565-591, 1970.

Geographical Survey Institute of Japan, Crustal deformation of Northern Shikoku accompanying the Nankaido earthquake of 1948, Jour. Geogr. Surv. Inst. of Japan, 4, 1948.

Geographical Survey Institute of Japan, Resurvey of the South-Western part of Japan after the Great Nankaido earthquake of 1946, Jour. Geogr. Surv. Inst. of Japan, 3, 31-118, 1952.

Geographical Survey Institute of Japan, Resurvey of the South-Western part of Japan after the Great Nankaido earthquake of 1946, Jour. Geogr. Surv. Inst. of Japan, 4, 1-69, 1954.

Geographical Survey Institute of Japan, Collection of results of precise levels along primary bench marks, 1, 1955.

Geographical Survey Institute of Japan, Index maps of precise leveling for every observation year, 1967.

Gutenberg, B., and C. F. Richter, Seismicity of the Earth and Associated Phenomena, Princeton Univ. Press, Princeton, N. J., pp. 310, 1954.

Hamilton, E. L., Marine geology of abyssal plains in the Gulf of Alaska, Jour. Geophys. Res., 72, 4189-4214, 1967.

Hamilton, R. M., Aftershocks of the Borrego Mountain, California, earthquake from April 12 to June 12, 1968, Bull. Seismol. Soc. Amer., in preporation ~~press, 1970~~.

Hastie, L. M., and J. C. Savage, A dislocation model for the 1964 Alaska earthquake, Bull. Seismol. Soc. Amer., 60, 1389-1392, 1970.

Hatori, T., Vertical displacement in a Tsunami source area and the topography of the sea bottom, Bull. Earthq. Res. Inst., 44, 1449-1464, 1966.

Hatori, T., Vertical crustal deformation and Tsunami energy, Bull. Earthq. Res. Inst., 48, 171-188, 1970.

Hayashi, T., A study of the vertical movements of the earth's crust by means of the precise leveling, Jour. Geod. Soc. Japan, 15, 1-69, 1970.

Heezen, B. C., and A. S. Laughton, Abyssal plains, in The Sea, Vol. III, edited by M. N. Hill, Interscience Pub., New York, 312-364, 1963.

Hilde, T. W. C., J. M. Wageman, and W. T. Hammond, The structure of Tosa Terrace and Nankai Trough off southeastern Japan, Deep-Sea Research, 16, 67-75, 1969.

Hofmann, R. B., Geodimeter fault movement investigations in California, Calif. Dept. Water Resources Bull., 116-6, 1968.

Huzita, L., Tectonic development of southwest Japan in the Quaternary period, Jour. Geosciences, Osaka City Univ., 12, 53-70, 1969.

Ichikawa, M., On the mechanism of the earthquakes in and near Japan during the period from 1950 to 1957, Geophys. Mag., 30, 355-403,

Ichikawa, M., The mechanism of earthquake occurring in central and southwest Japan, and some related problems, Papers in Meteorology and Geophysics, 56, 104-156, 1965.

Isacks, B., Focal Mechanisms of Earthquakes in Western South America, Trans. Am. Geophy. Union, 51, 355, 1970.

Isacks, B. L., L. R. Sykes, and J. Oliver, Focal mechanisms of deep and shallow earthquakes in the Tonga and Kermadec Island Arcs, Geol. Soc. Amer. Bull., 80, 1443-1470, 1969.

Isacks, B. L., J. Oliver and L. R. Sykes, Seismicity and the new global tectonics, J. Geophys. Res., 73, 5855-5899, 1968.

Imamura, A., On the seismic activity of central Japan, Jap. Jour. Astro. & Geophys., 6, 119-137, 1928.

Imamura, A., On the chronic and acute earth-tilting in the Kii Peninsula, Jap. Jour. Astro. & Geophys., 7, 31-45, 1929.

Imamura, A., On the chronic and acute earth-tilting in the southern part of Shikoku, Jap. Jour. Astro. & Geophys., 8, 29-37, 1930.

Kanamori, H., Seismological evidence for a lithospheric normal faulting - the Sanriku earthquake of 1933, Bull. Earthq. Res. Inst., in press, 1970.

Kaneko, S., Rising promontories associated with a subsiding coast and sea-floor in south-western Japan, Trans. Roy. Soc. New Zealand, 4, 211-228, 1966A.

Kaneko, S., Transcurrent displacement along the Median Line, south-western Japan, New Zealand J. Geol. Geophys., 9, 45-59, 1966B.

Karig, D. E., Structural history of the Mariana Island Arc system, Geol. Soc. Amer. Bull., in press, 1971.

Kasahara, K., Physical condition of earthquake faults as deduced from geodetic data, Bull. Earthq. Res. Inst., 36, 455-464, 1958.

Katsumata, M. and L. R. Sykes, Seismicity and tectonics of the western

Pacific: Izu-Mariana Caroline and Ryukyu-Taiwan regions, J. Geophys. Res., 74, 5923-5948, 1969.

Kawasumi, H., Measures of earthquake danger and expectancy of maximum intensity throughout Japan as inferred from the seismic activity in historical times, Bull. Earthq. Res. Inst., 29, 469-482, 1951.

Le Pichon, X., Sea floor spreading and continental drift, J. Geophys. Res., 73, 3661-3705, 1968.

Love, A. E. H., The Mathematical Theory of Elasticity, 643 pp., Dover Press, New York, 1944.

Matsuda, T., K. Nakamura, and A. Sugimura, Late Cenozoic orogeny in Japan, Tectonophysics, 4, 349-366, 1967.

Matuzawa, T., Study of Earthquakes, Uno Shoten, 213 pp., Tokyo, Japan, 1964.

Mansinha, L. and D. E. Smylie, Displacement fields of inclined faults, J. Geophys. Res., in press, 1970.

Maruyama, T., Statical elastic dislocations in an infinite and semi-infinite medium, Bull. Earthq. Res. Inst., 42, 289-368, 1964.

McKenzie, D. P. and R. L. Parker, The North Pacific: An example of tectonics on a sphere, Nature, 216, 1276-1280, 1967.

McKenzie, D. P. and W. J. Morgan, Evolution of triple junctions, Nature, 224, 125-133, 1969.

Minato, M., M. Gorai, and M. Hunahashi, (editors), The Geologic Development of the Japanese Islands, 442 pp., Tsukiji Shokan Co., 1965.

Miyabe, N., Vertical earth movements in Nankai District, Bull. Geogr. Surv. Inst., 4, 1-14, 1955.

Miyashiro, A., Orogeny, regional metamorphism and magmatism in the Japanese Islands, Medd. Dan. Geol. Foren., 17, 390- , 1967.

Mogi, K., Development of aftershock areas of great earthquakes, Bull. Earthq. Res. Inst., 46, 175-203, 1968.

Mogi, K., Recent horizontal deformation of the earth's crust and tectonic activity in Japan (1), Bull. Earthq. Res. Inst., 48, 413-430, 1970.

Molnar, P., and L. R. Sykes, Tectonics of the Caribbean and Middle America regions from focal mechanisms and seismicity, Geol. Soc. Amer. Bull., 80, 1639-1684, 1969.

Morgan, W. J., Rises, trenches, great faults and crustal blocks, J. Geophys. Res., 73, 1959-1982, 1968.

National Aeronautics and Space Administration, The terrestrial environment solid-earth and ocean physics application of space and astronomics techniques, Report of a Study at Williamstown, Mass., August 1969.

Nagata, T., and A. Okada, Land deformation of the Muroto Point before and after the Nankai great earthquake on December 21, 1946, Bull. Earthq. Res. Inst., 25, 85-89, 1947.

Okada, A., and T. Nagata, Land deformation of the neighborhood of Muroto Point after the Nankaido great earthquake in 1946, Bull. Earthq. Res. Inst., 31, 169-177, 1953.

Okada, A., Land deformation of the southern part of the Kii Peninsula, southwest Japan, Bull. Earthq. Res. Inst., 38, 113-124, 1960.

Omote, S., On the central area of seismic sea waves, Bull. Earthq. Res. Inst., 25, 15-19, 1947.

Parkin, E. J., Horizontal crustal movements determined from surveys after the Alaskan earthquake of 1964, the Prince William Sound, Alaska, earthquake of 1964 and aftershocks, United States Government Printing Office, 35-98, 1969.

Plafker, G. and M. Rubin, Vertical tectonic displacements in south-central Alaska during and prior to the great 1964 earthquake, Jour. Geosciences, Osaka City Univ., 10, 53-66, 1967.

Plafker, G., Tectonics of the March 1964 Alaska earthquake, Geological Survey Professional Paper, 543-I, 74 pp., 1969.

Plafker, G. and J. C. Savage, Mechanism of the Chilean earthquakes of May 21 and 22, 1960, Geol. Soc. Amer., 81, 1001-1030, 1970.

Reid, H. F., The mechanics of the earthquake in the California earthquake of April 18, 1906, Report on the State Earthquake Investigation Commission, 2, 192 pp., Carnegie Institution of Washington, D. C., 1910.

Richter, C. F., Elementary Seismology, 768 pp., W. H. Freeman and Co., San Francisco, 1958.

Savage, J. C., and L. M. Hastie, Surface deformation associated with dip-slip faulting, J. Geophys. Res., 71, 4897-4904, 1966.

Savage, J. C. and L. M. Hastie, A dislocation model for the Fairview Peak, Nevada, earthquake, Bull. Seismol. Soc. Amer., 59, 1937-1948, 1969.

Sawamura, T., Relation between the activities of the outer earthquake zone in south-western Japan and the geologic structure and crustal movements of Shikoku and its vicinity, Research Reports of Kochi University, 2, 1-46, 1953.

Sawamura, T., On the Nankai thrust and the distribution of initial motions of seismic waves by the Nankai earthquake in 1946, Research Reports of Kochi University, 3, 1-6, 1954.

Scholz, C. H., M. Wyss, and S. W. Smith, Seismic and aseismic slip on the San Andreas fault, J. Geophys. Res., 74, 2049-2069, 1969.

Scholz, C. H., and T. J. Fitch, Strain and creep along the San Andreas fault, J. Geophys. Res., 74, 6649-6666, 1969.

Scholz, C. H., and T. J. Fitch, Strain and creep in central California, J. Geophys. Res., 75, 4447-4453, 1970.

Stauder, W., S. J. and G. A. Bollinger, The S-wave project for focal mechanism studies, earthquakes of 1962, Bull. Seismol. Soc. Amer., 54, 2198-2208, 1964.

Stauder, W., S. J., and G. A. Bollinger, The S-wave project for focal mechanism studies, earthquakes of 1963, Bull. Seismol. Soc. Amer., 56, 1363-1371, 1966a.

Stauder, W., S. J., and G. A. Bollinger, The Focal mechanism of the Alaska earthquake of March 28, 1964, and of its aftershock sequence, J. Geophys. Res., 71, 5283-5296, 1966b.

Stauder, W., S. J., Mechanism of the Rat Island earthquake sequence of February 4, 1965, with relation to island arcs and sea-floor spreading, J. Geophys. Res., 73, 3847-3859, 1968a.

Stauder, W., S. J., Tensional character of earthquake foci beneath the Aleutian trench with relation to sea-floor spreading, J. Geophys. Res., 73, 7693-7702, 1968b.

Stekette, J. A., On Volterra, dislocations in a semi-infinite medium, Can. J. Phy., 36, 192-205, 1958.

Sugimura, A., and Y. Naruse, Changes in sea level, seismic upheavals, and coastal terraces in southern Kanto region, Japan (I), Japan J. Geol. Geogr., 14, 101-113, 1954.

Sugimura, A., and Y. Naruse, Changes in sea level, seismic upheavals, and coastal terraces in the southern ~~Kuito~~ Kanto region, Japan (II), Japan J. Geol. Geogr., 15,165-176, 1955.

Sugimura, A., and S. Uyeda, Island Arcs: Japan and its environrons, in

(Continued on page 75)

Phys. and Chemistry of the Earth, in press, 1970.

Tsuboi, C., Investigation of the deformation of the earth's crust found by precise geodetic means, Jap. Jour. Astro. & Geophys., 10, 93-248, 1933.

Utsu, T., Magnitude of earthquake and occurrence of their aftershocks, Zisin., 10, 35-54, 1957.

Walsh, J. B., Dip angle of faults as calculated from surface deformation, J. Geophys. Res., 74, 2070-2080, 1969.

Watanabe, A., The geomorphology of the coastal district of south-eastern Shikoku; a contribution to the knowledge of the recent crustal movements of the area under discussion, Bull. Earthq. Res. Inst., 10, 209-233, 1932.

Watanabe, A., The geomorphology of the coastal districts of the southern part of Shikoku Island and its bearing on the crustal deformations accompanying the great Nankai earthquakes, Bull. Geogr. Surv. Inst., 1, 37-72, 1948.

Watanabe, A., Geomorphology in relation to recent crustal movements in Japan, in Proceedings of I. G. U. Regional Conference in Japan 1957, 215-221, 1959.

Whitten, C. A., Horizontal earth movements, vicinity of San Francisco, California, Trans. Amer. Geophys. Union, 29, 318-328, 1948.

Whitten, C. A., Measurements of earth movements in California, Calif. Div. Mines Bull., 171, 75, 1955.

Whitten, C. A., Remeasurement of triangulation net in vicinity of San

Francisco in San Francisco earthquake of March 1957, Calif. Div. Mines Spec. Rep., 57, 56-57, 1958.

Whitten, C. A., Horizontal movement in the earth's crust, J. Geophys. Res., 65, 2839-2844, 1960.

Yamaguti, S., On the changes in the heights of yearly mean-sea-levels in recent years, Bull. Earthq. Res. Inst., 46, 901-906, 1968a.

Yamaguti, S., On the changes in the heights of yearly mean-sea-levels preceding the great earthquake, Bull. Earthq. Res. Inst., 46, 1269-1273, 1968b.

Yonekura, N., Geomorphic development and mode of crustal movement on the south coast of Kii Peninsula, southwestern Japan, Jour. Geogr., 77, 1-23, 1968.

Yoshikawa, T., S. Kaizuka, and Y. Ota, Crustal movement in the late Quaternary revealed with coastal terraces on the southeast coast of Shikoku, southwestern Japan, Jour. Geod. Soc. Jap., 10, 116-122, 1964.

Yoshikawa, T., On the relations between Quaternary tectonic movement and seismic crustal deformation in Japan, Bull. Dept. Geogr. Univ. Tokyo, 2, 1-24, 1970.

TABLE I[illegible]

Least Square Solutions to Leveling Data in Region A

(Eastern Shikoku)[t]

Dip (degrees)	Slip (meters)	H (km)	R (km)	Standard Deviation (mm)
10	3	34	69	168
20	3	57	43	101
25	4	71	29	83
30	5	82	17	72
35	7	86	8	67
40	10	87	14	67
45	17	88	-10	69
50	40	96	-35	80

t Fault constrained to intersect the free surface

Fault strike fixed at N70°E

Half length 160 km

Origin of coordinates 135.1°E, 32.8°N

H Down-dip length of fault plane

R Horizontal translation of fault plane perpendicular to strike relative to the origin of coordinates (Positive direction is NNW)

TABLE II

Least Square Solutions to Leveling Data in Region C

(Western Shikoku)[t]

Dip (degrees)	Slip (meters)	H (km)	R (km)	Standard Deviation
20	8	213	-120	51
30	13	145	-60	48
35	18	113	-28	47
40	24	110	-35	49
45	41	112	-49	63

t Fault constrained to intersect the free surface

Fault strike fixed at N70°E

Half length 160 km

Origin of coordinates 135.1°E, 32.8°N

H Down-dip length of fault plane

R Horizontal translation of fault plane perpendicular to strike relative to the origin of coordinates (Positive direction is NNW)

TABLE III

Least Square Solutions to Leveling Data[t]

Region	Time	Slip*(meters)	H (km)	Standard Deviation (mm)	Remarks
A	34 yrs. pre-earthquake (approx. 1896-1930)	-1 (-3)	111	29	
	1929-June 1947	7	94	68	
	1929-1964	4	124	83	
B	1937-Sept. 1947	11	97	76	
C	34 yrs. pre-earthquake (approx. 1896-1930)	-4 (-12)	86	33	
	1939-Aug. 1947	18	88	62	
	1948-1950	-11	48	58	All data pts. included
	1948-1950	-5	70	30	Only uplift data
	1950-1964	-7	55	24	All data pts. included
	1950-1964	-6	59	15	Only uplift data
	1939-1950	15	93	84	
Kii	34 yrs. pre-earthquake (approx. 1896-1930)	-1/2 (-1 1/2)	89	30	
	1928-1947	6	55	58	

t Fault constrained to intersect the surface
Strike fixed at N70°E; Dip fixed at 35°
Half length 160 km
Origin of coordinates 135.1°E, 32.8°N

* Negative slip corresponds to virtual slip during periods of strain accumulation or real slip during backsliding

H Down-dip length of fault plane

( ) Virtual slip accumulated during an average recurrance interval between Nankaido earthquakes of 100 years

TABLE IV

Tilts of Southeastern Peninsula of Shikoku[t]

(including Muroto Point)

Tilt* mm/km	Tilt* sec of arc	Deformation	Time	Data
-7.0	-1.4	Strain	1896-1929	Leveling[1]
-8.5	-1.7	Strain	1896-1935	Leveling[1]
29.0	5.7	18 yrs strain plus earthquake (including permanent tilt) and 2 months of post-earthquake adjustments	1929-Feb. 1947	Leveling[1]
26.2	5.3	32 yrs strain plus earthquake and 3 yrs of post-earthquake adjustments	1929-1964	Leveling[1]
-18.6	-3.8	Total strain	89 yrs from 1857 (3 yrs after previous Nankaido eq.) to Dec. 1946.	Extrapolated from leveling
31.8	6.5	Earthquake (including permanent tilt)	Nankaido earthquake	Extrapolated from leveling
13.0	2.7	Permanent tilt	Nankaido earthquake	Extrapolated from leveling
6	1	Permanent tilt	100 yrs (out of 90,000)	Lower Muroto-Misaki Terraces[2]
6	1	Permanent tilt	100 yrs (out of 170,000)	Lower Hane-saki Terraces[2]

t Only data from western side of promontory, negative tilt is toward SE.

* Projected on a plane striking N20°W, i.e., perpendicular to the strike of the fault.

1 Geographical Survey Institute of Japan (1955) and unpublished results of the 1964 survey (Okada, personal communication)

2 Yoshikawa, Kaizuka and Ota (1964).

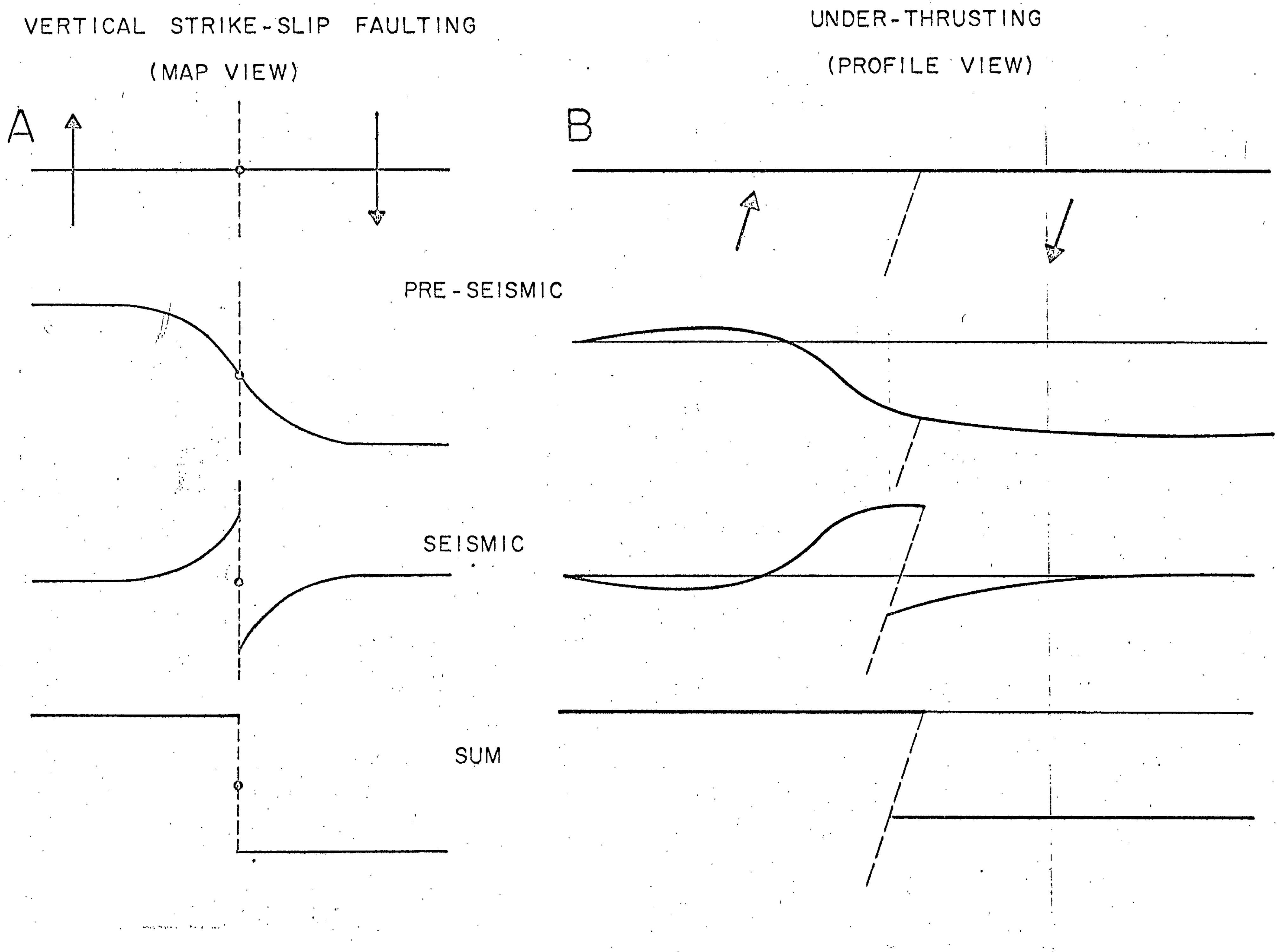

VERTICAL STRIKE-SLIP FAULTING
(MAP VIEW)
UNDER-THRUSTING
(PROFILE VIEW)
A
B
PRE-SEISMIC
SEISMIC
SUM

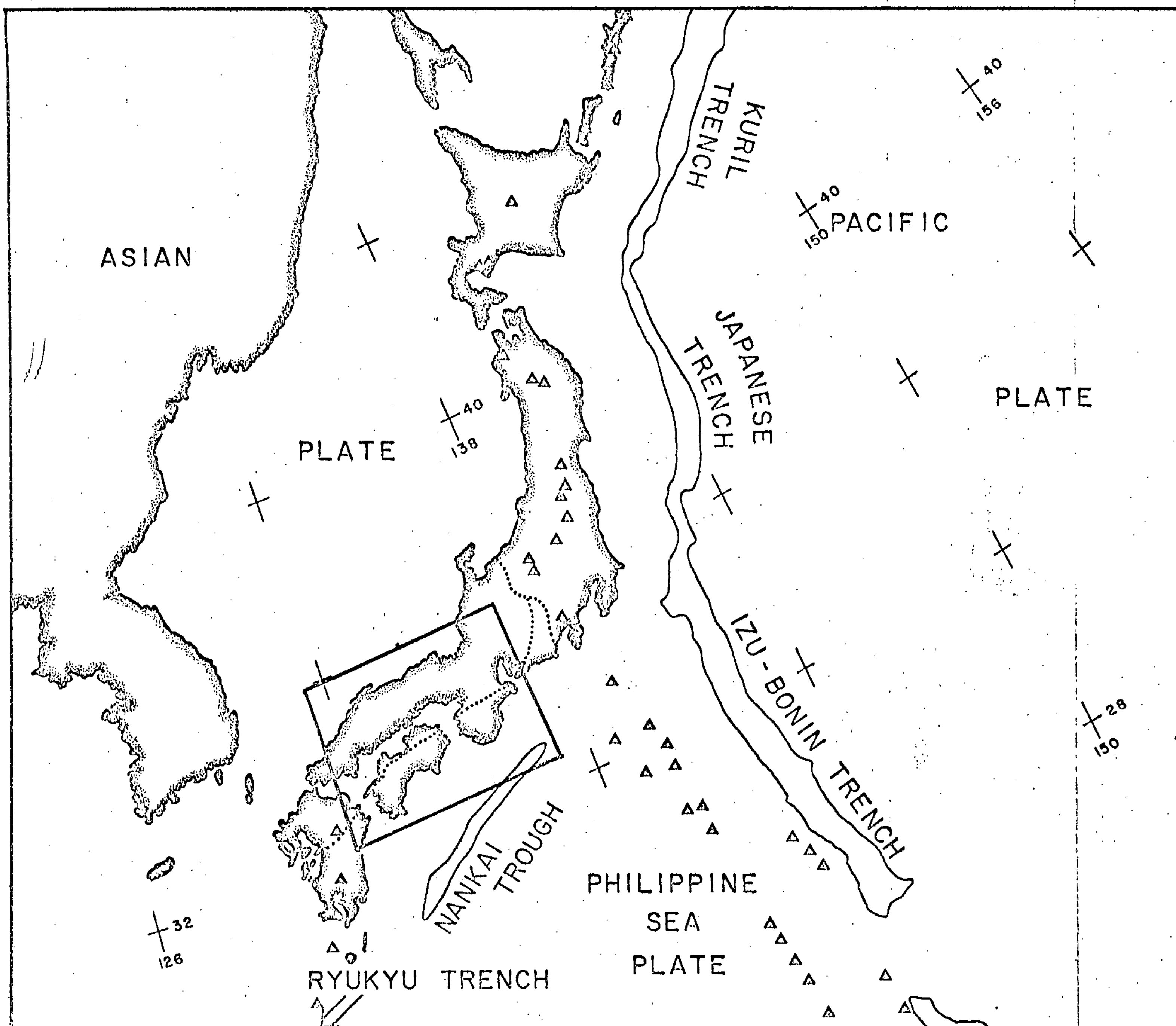
ASIAN
PLATE
KURIL TRENCH
JAPANESE TRENCH
PACIFIC
PLATE
IZU-BONIN TRENCH
NANKAI TROUGH
PHILIPPINE
SEA
PLATE
RYUKYU TRENCH
40
156
40
150
40
138
28
150
32
126

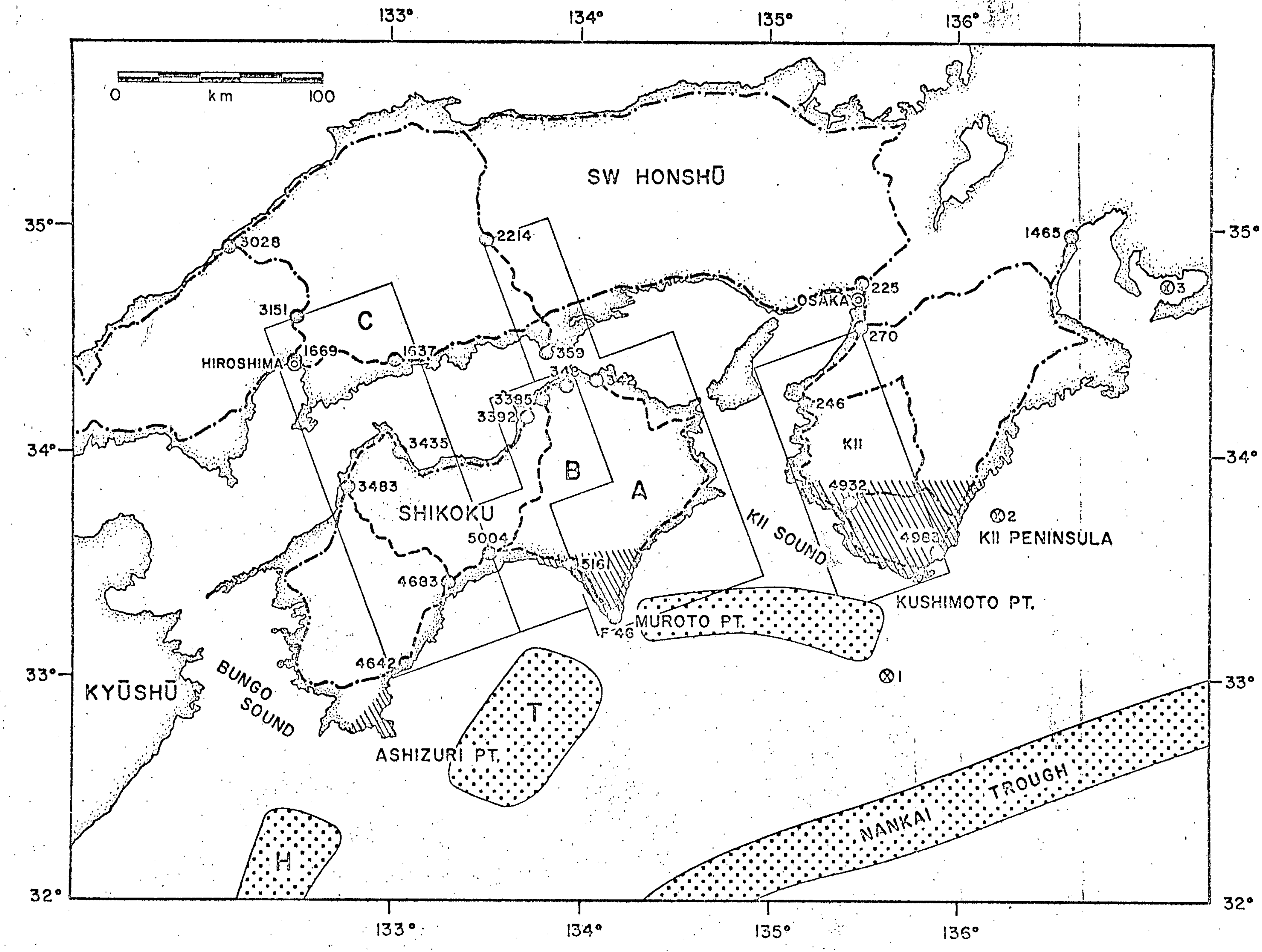

133°
134°
135°
136°
35°
34°
33°
32°
0 km 100
SW HONSHŪ
3028
2214
1465
3151
C
HIROSHIMA
1669
1637
359
340
342
3395
3392
3435
B
A
225
OSAKA
270
246
KII
4932
4963
KII PENINSULA
3483
SHIKOKU
5004
4683
516
F46
MUROTO PT.
KII SOUND
KUSHIMOTO PT.
4642
KYŪSHŪ
BUNGO SOUND
ASHIZURI PT.
T
H
NANKAI TROUGH
⊗1
⊗2
⊗3

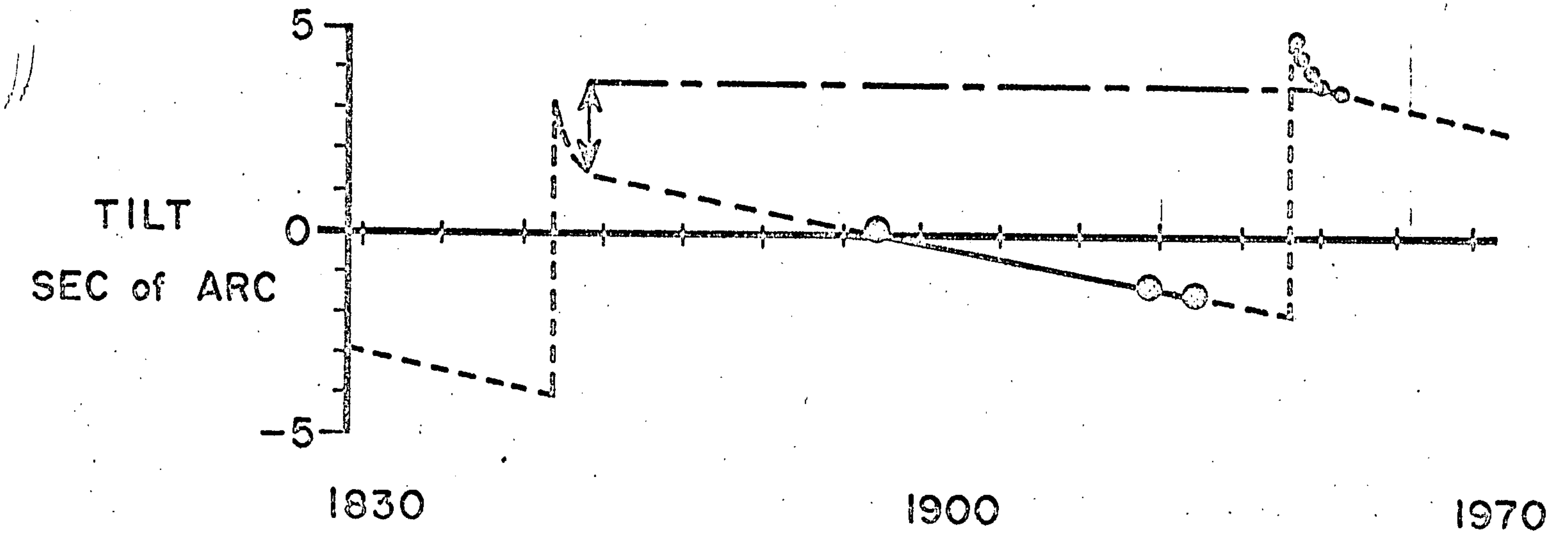

5
0
-5
TILT
SEC of ARC
1830
1900
1970

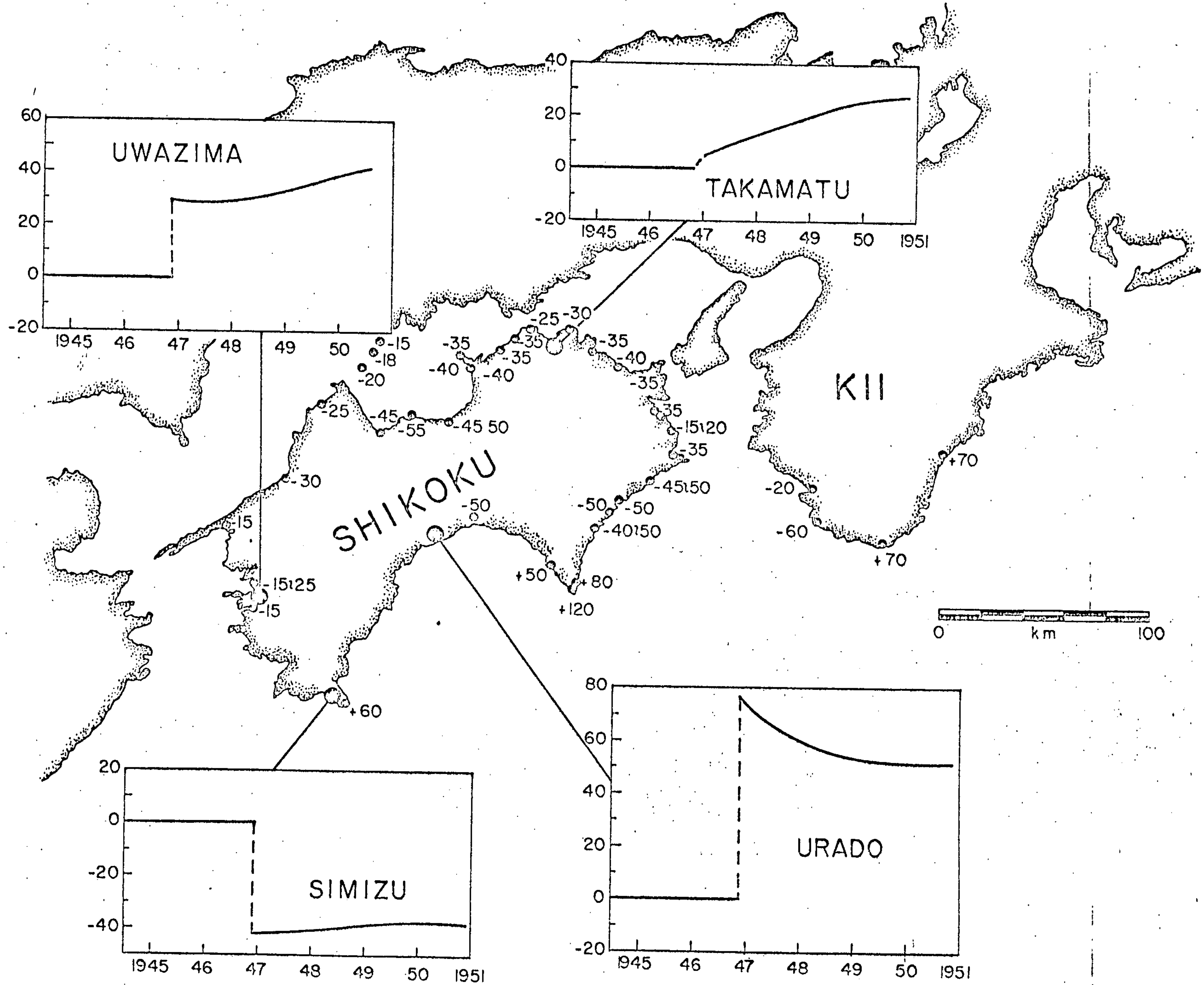

UWAZIMA
TAKAMATU
SIMIZU
URADO
SHIKOKU
KII
1945
46
47
48
49
50
1951
0
km
100
-15
-18
-20
-25
-30
-35
-40
-45
-55
-45 50
-15120
-45150
-50
-40150
+50
+80
+120
-15125
-15
+60
+70
-20
-60

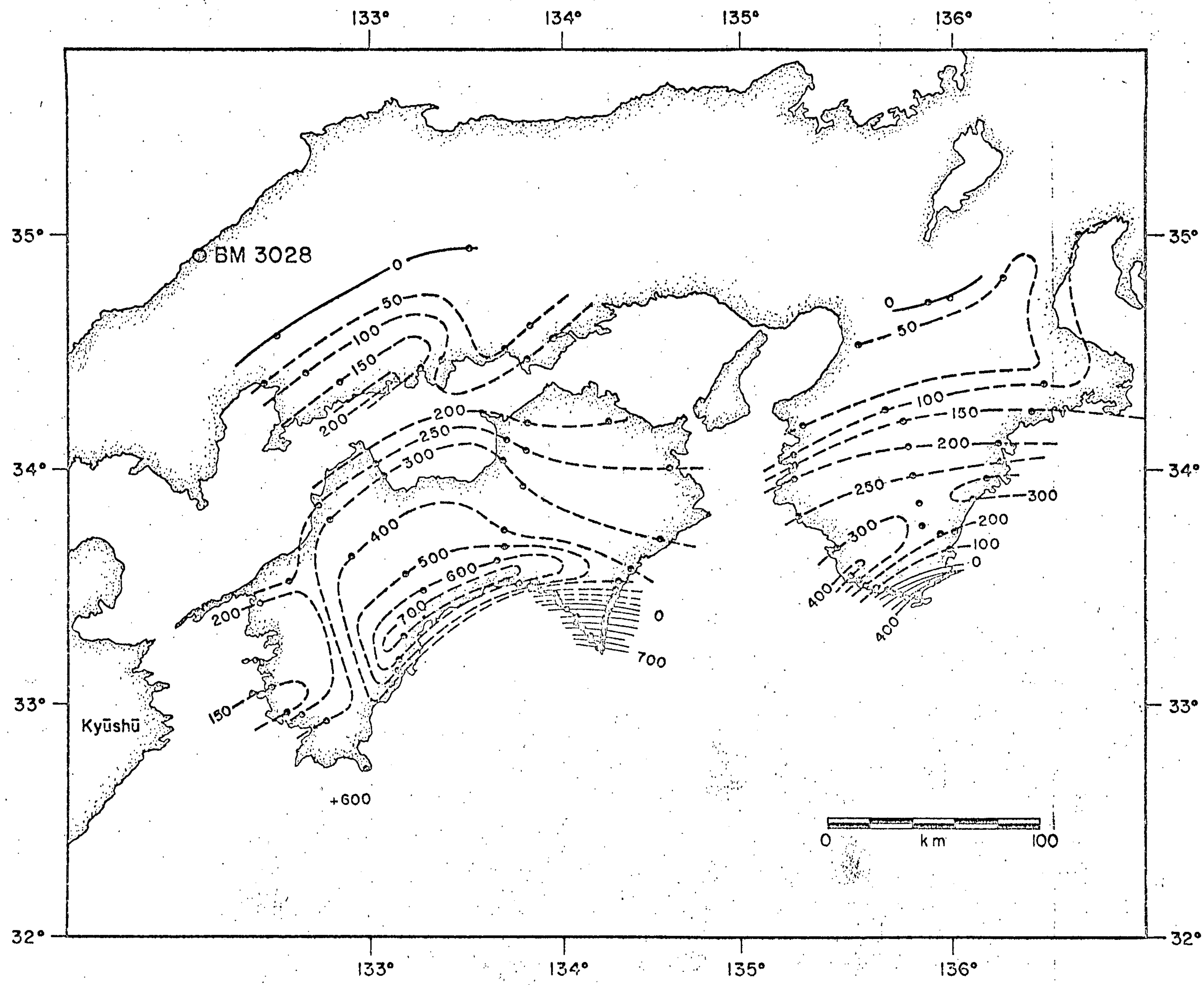
133°
134°
135°
136°
35°
34°
33°
32°
BM 3028
Kyūshū
0
50
100
150
200
250
300
400
500
600
700
+600
0 km 100

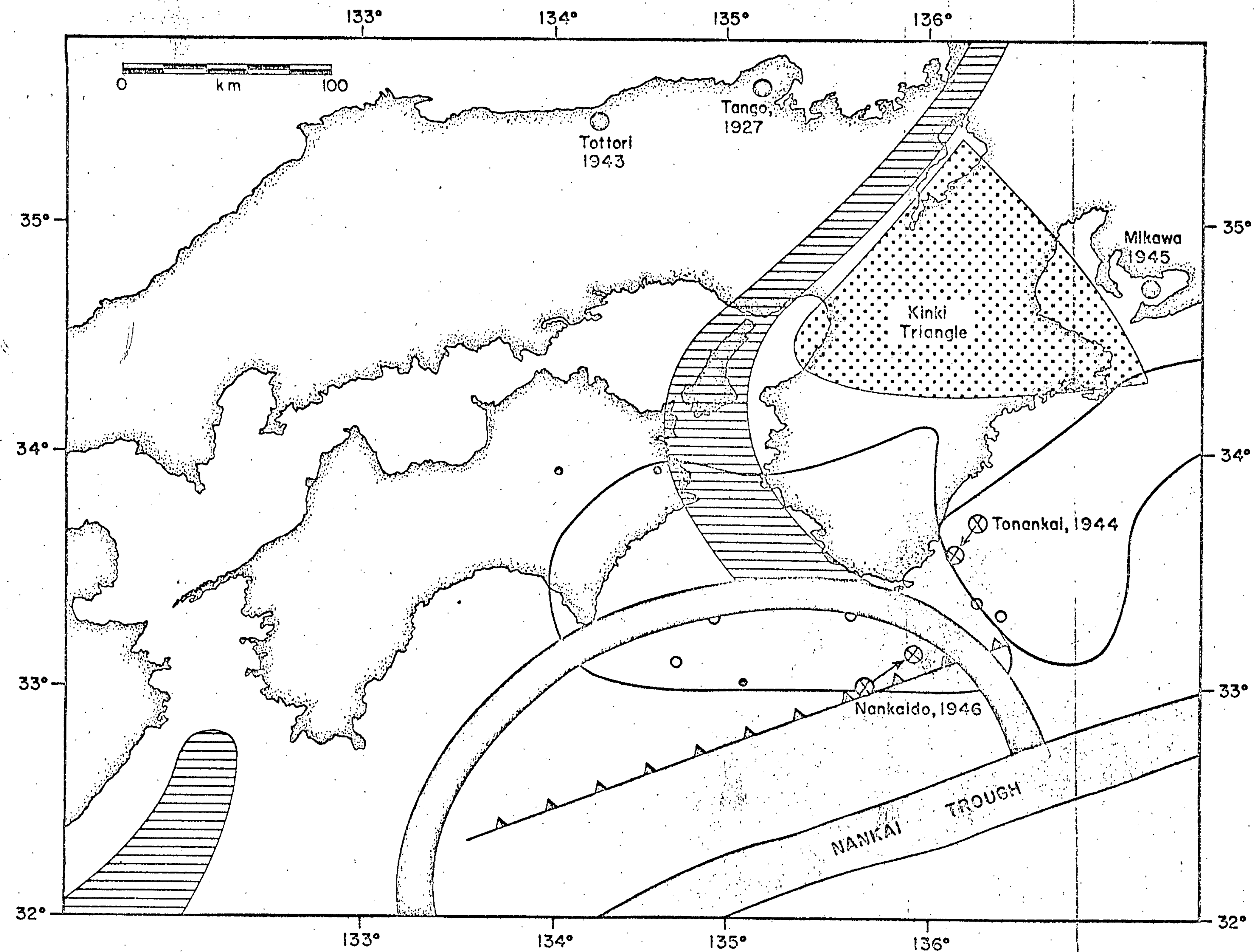

133°
134°
135°
136°
0 km 100
Tottori 1943
Tango, 1927
Mikawa 1945
Kinki Triangle
Tonankai, 1944
Nankaido, 1946
NANKAI TROUGH
35°
34°
33°
32°

A

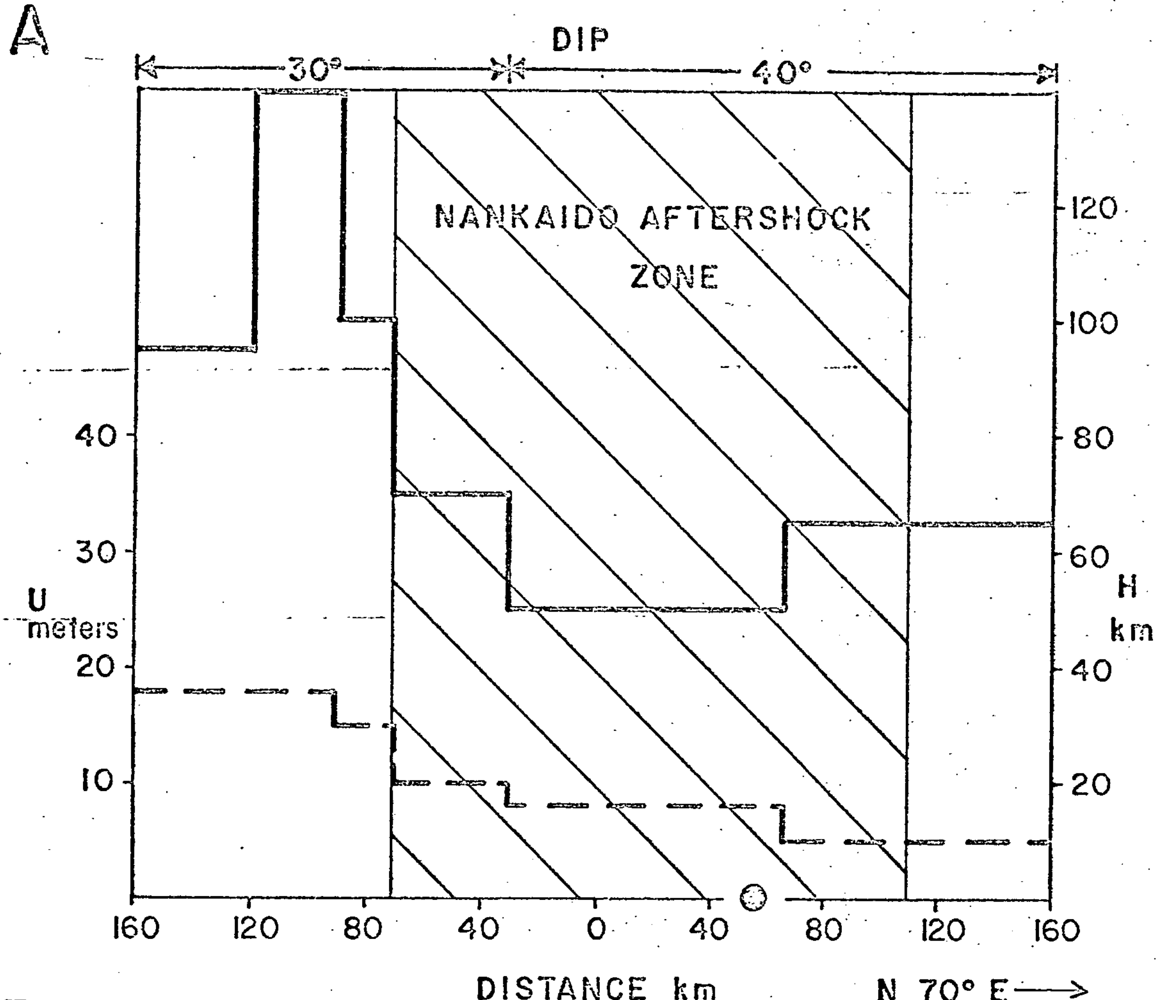
DIP
30°
40°
NANKAIDO AFTERSHOCK
ZONE
U
meters
H
km
40
30
20
10
120
100
80
60
40
20
160
120
80
40
0
40
80
120
160
DISTANCE km
N 70° E

B

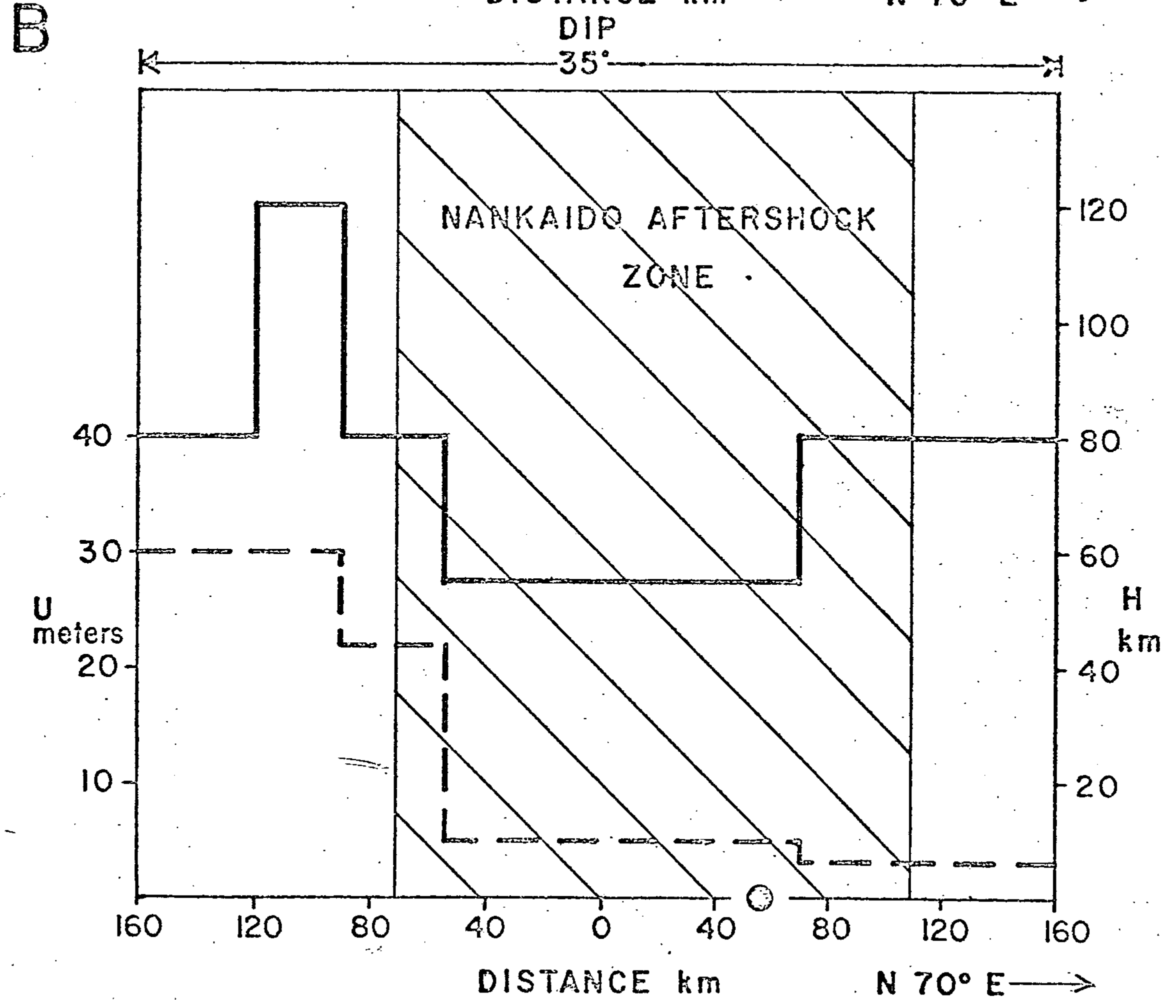
DIP
35°
NANKAIDO AFTERSHOCK
ZONE
U
meters
H
km
40
30
20
10
120
100
80
60
40
20
160
120
80
40
0
40
80
120
160
DISTANCE km
N 70° E

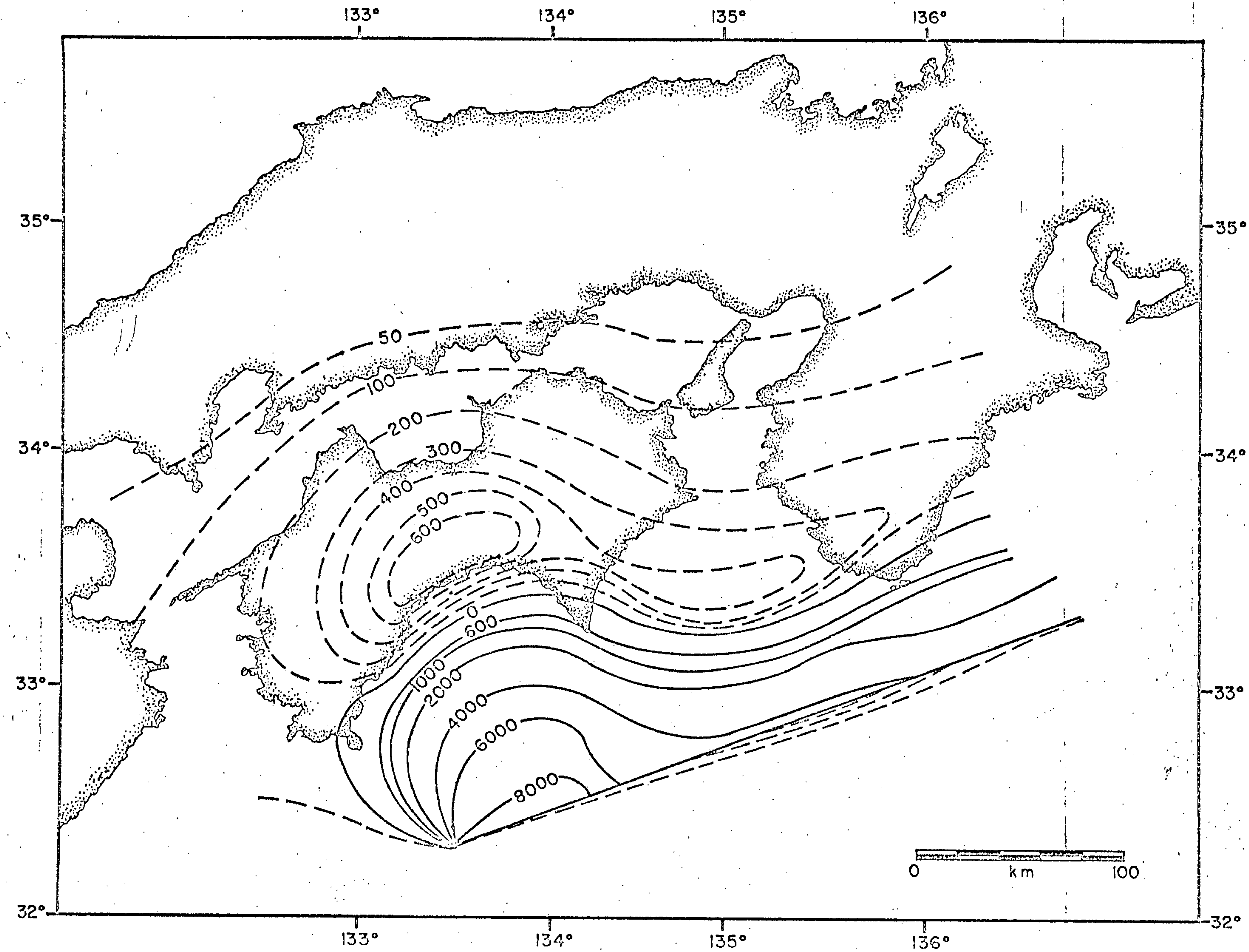

133°
134°
135°
136°
35°
34°
33°
32°
50
100
200
300
400
500
600
0
600
1000
2000
4000
6000
8000
0
km
100

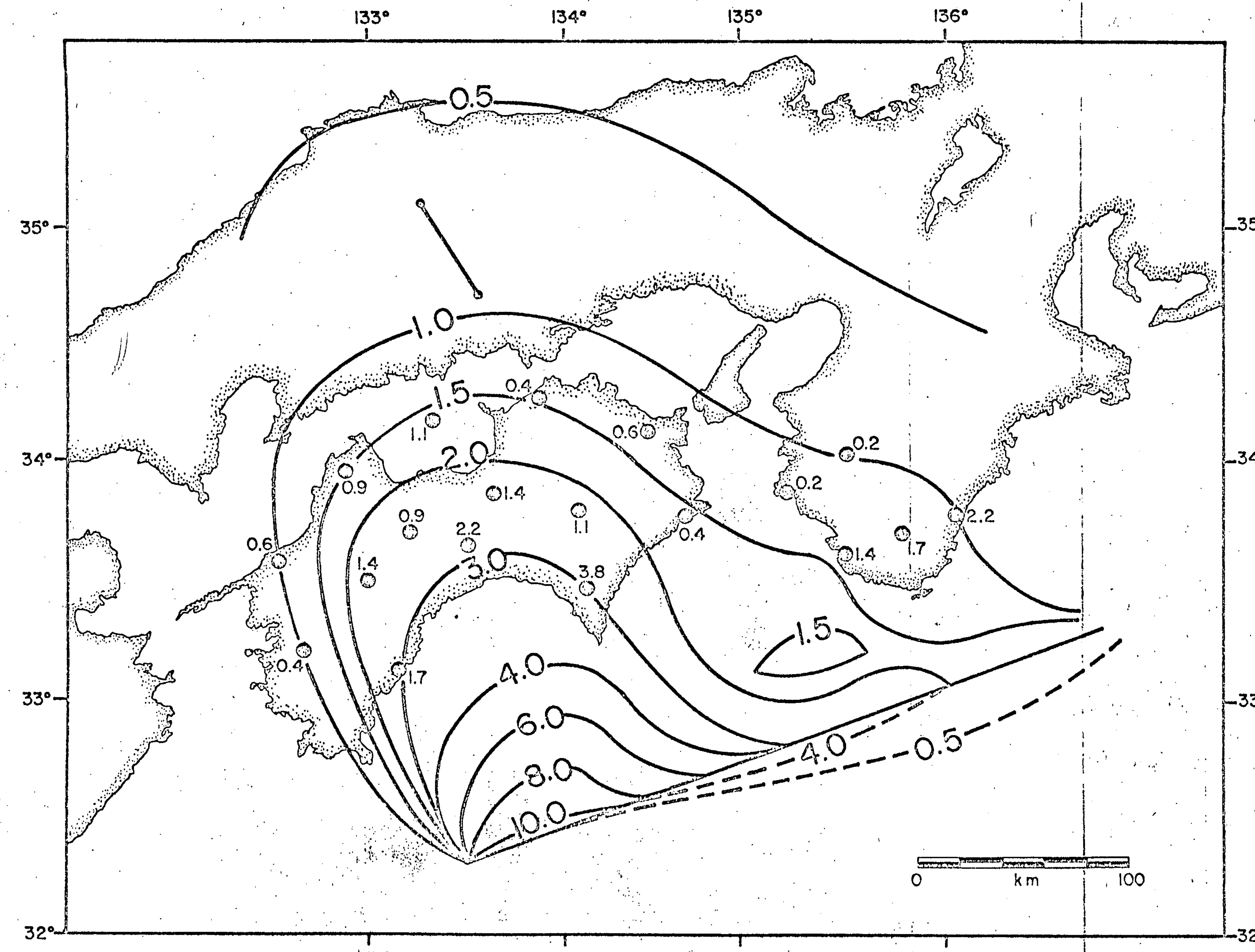

133°
134°
135°
136°
35°
34°
33°
32°
0.5
1.0
1.5
2.0
3.0
4.0
6.0
8.0
10.0
1.5
4.0
0.5
0.4
1.1
0.6
0.2
0.9
1.4
0.2
0.9
2.2
1.1
0.4
2.2
0.6
1.4
3.8
1.4
1.7
0.4
1.7
0 km 100

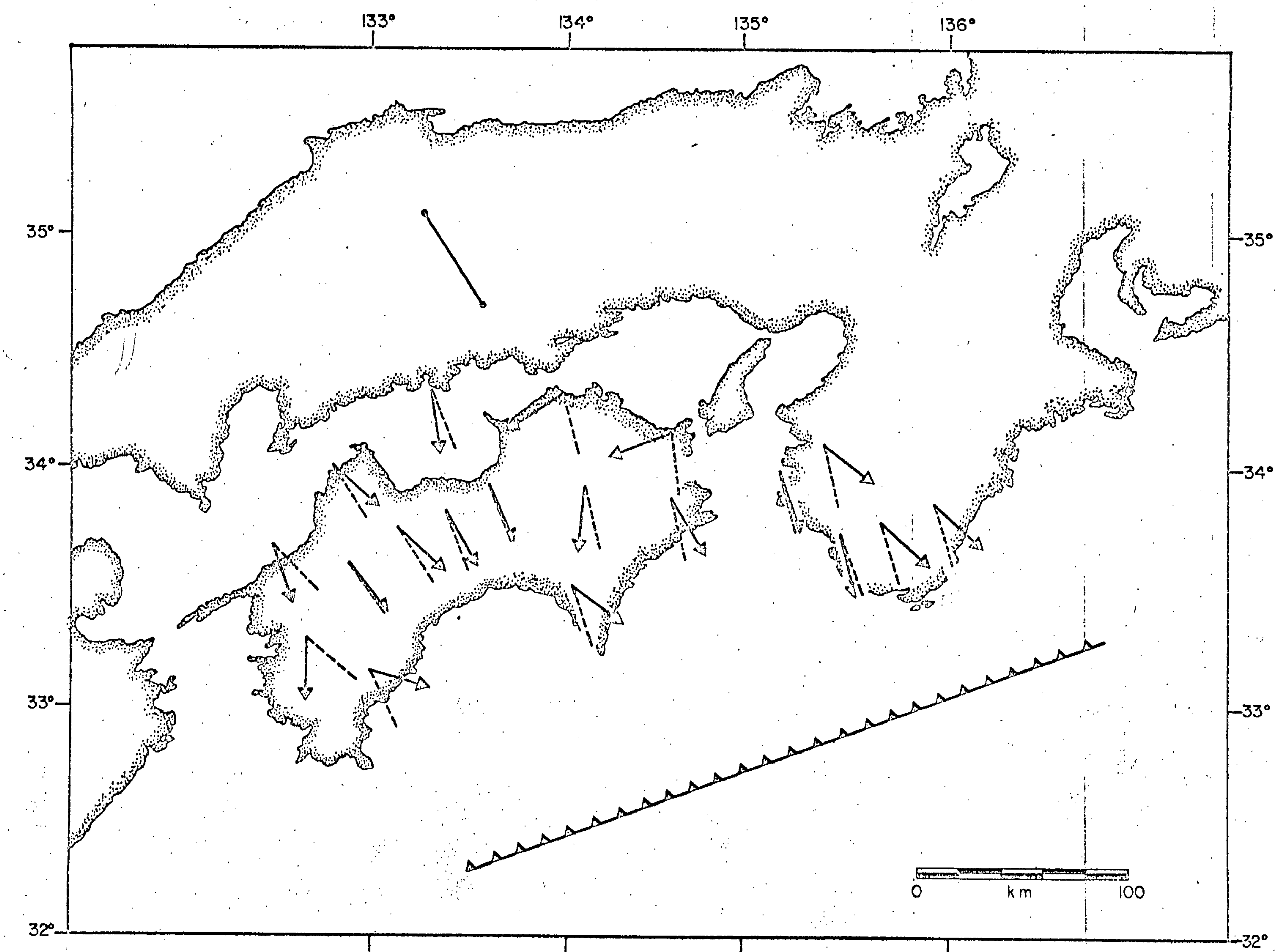
133°
134°
135°
136°
35°
34°
33°
32°
0 km 100

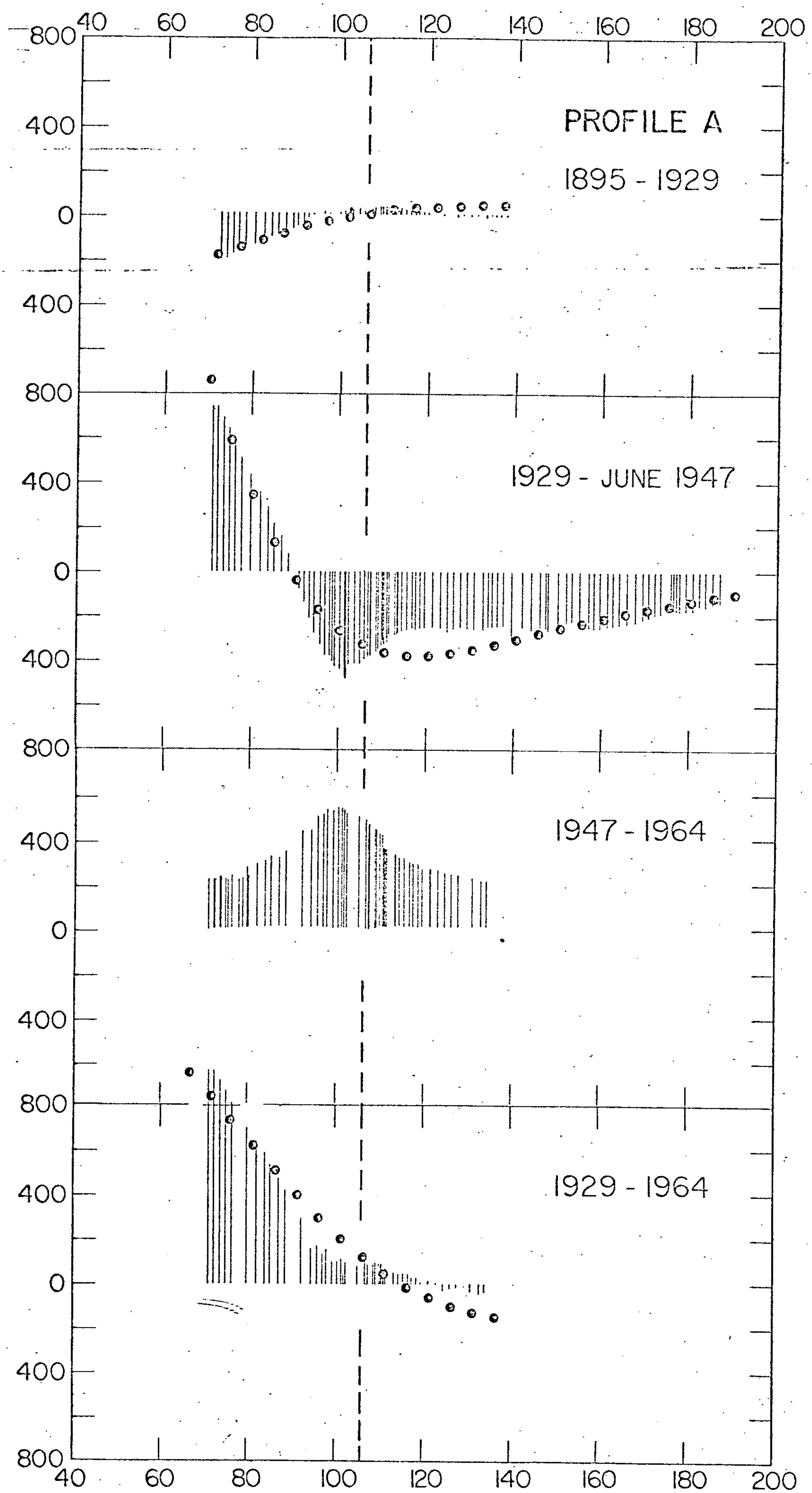
PROFILE A
1895 - 1929
1929 - JUNE 1947
1947 - 1964
1929 - 1964
40
60
80
100
120
140
160
180
200
800
400
0
400
800

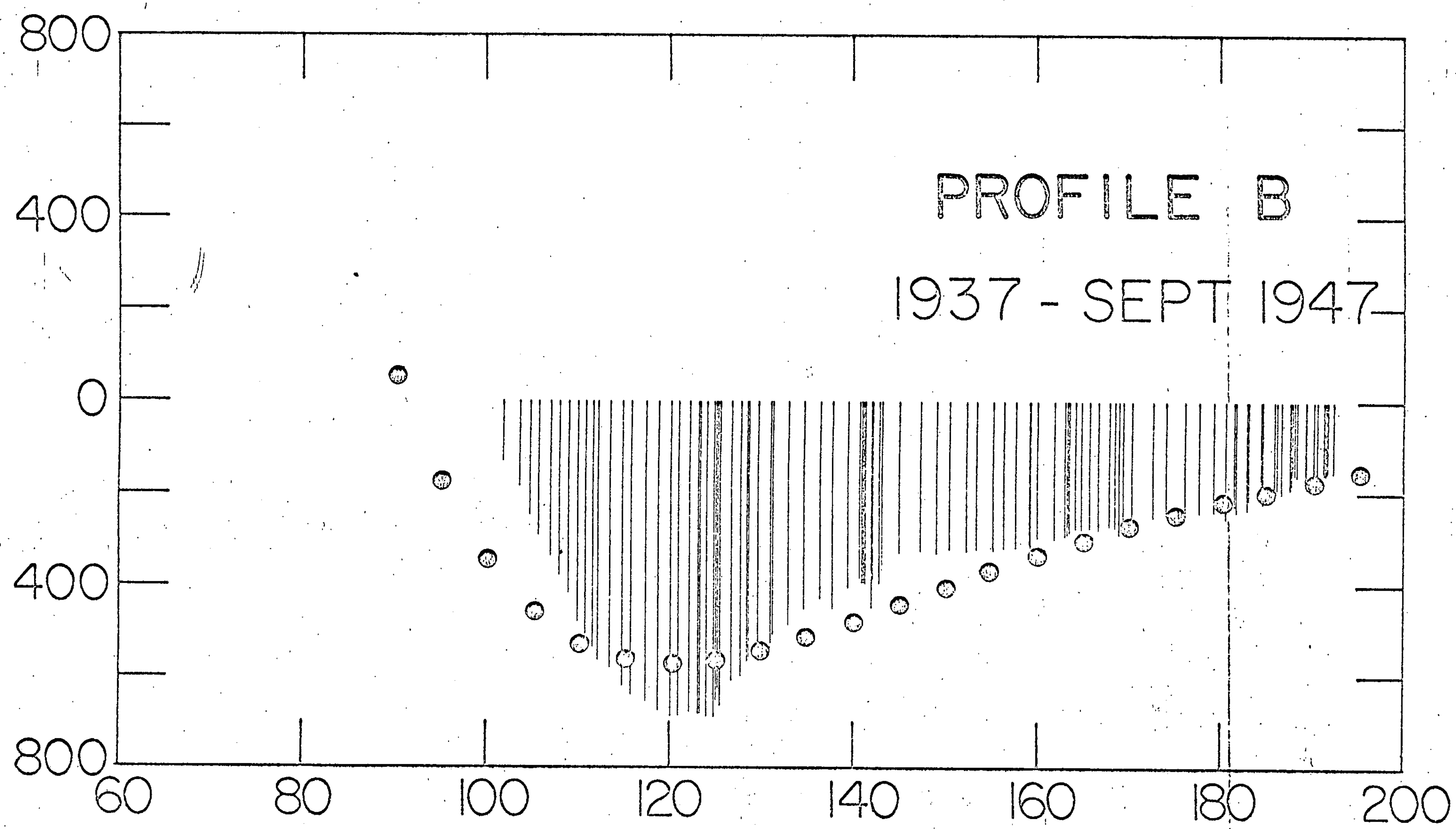
PROFILE B
1937 - SEPT 1947
800
400
0
400
800
60
80
100
120
140
160
180
200

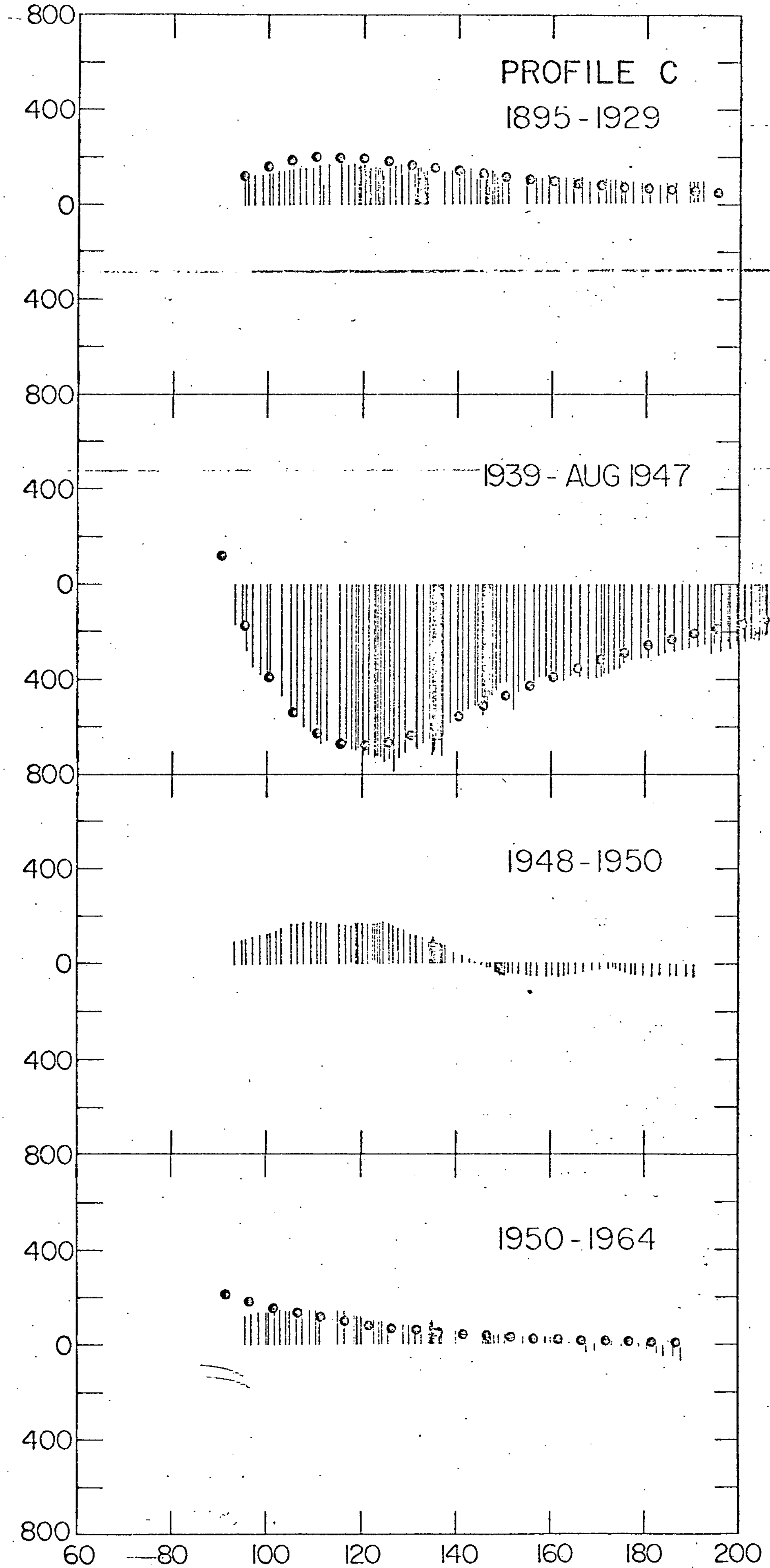
PROFILE C
1895 - 1929
1939 - AUG 1947
1948 - 1950
1950 - 1964
800
400
0
400
800
60
80
100
120
140
160
180
200

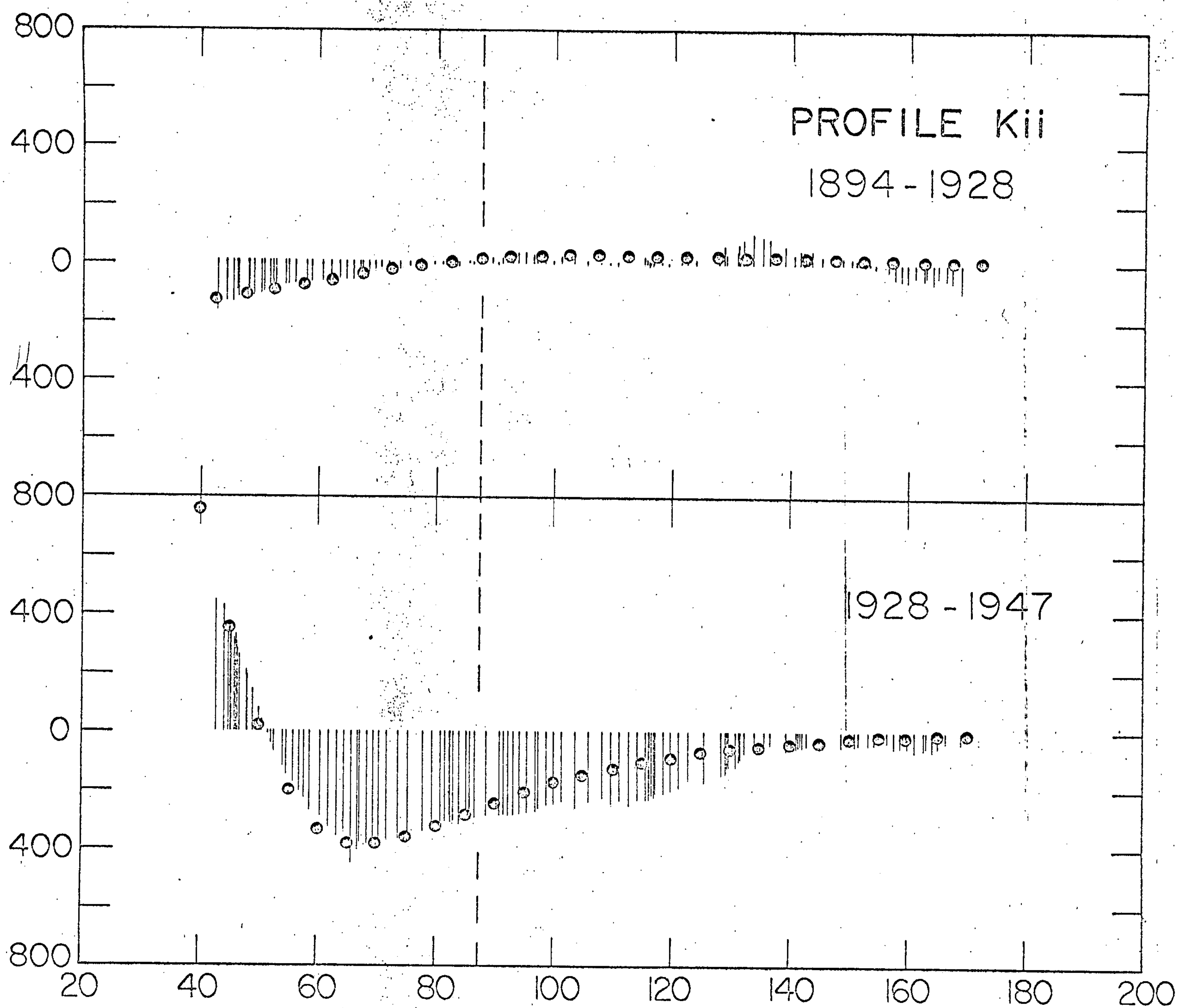
PROFILE Kii
1894 - 1928
1928 - 1947
800
400
0
400
800
400
0
400
800
20
40
60
80
100
120
140
160
180
200

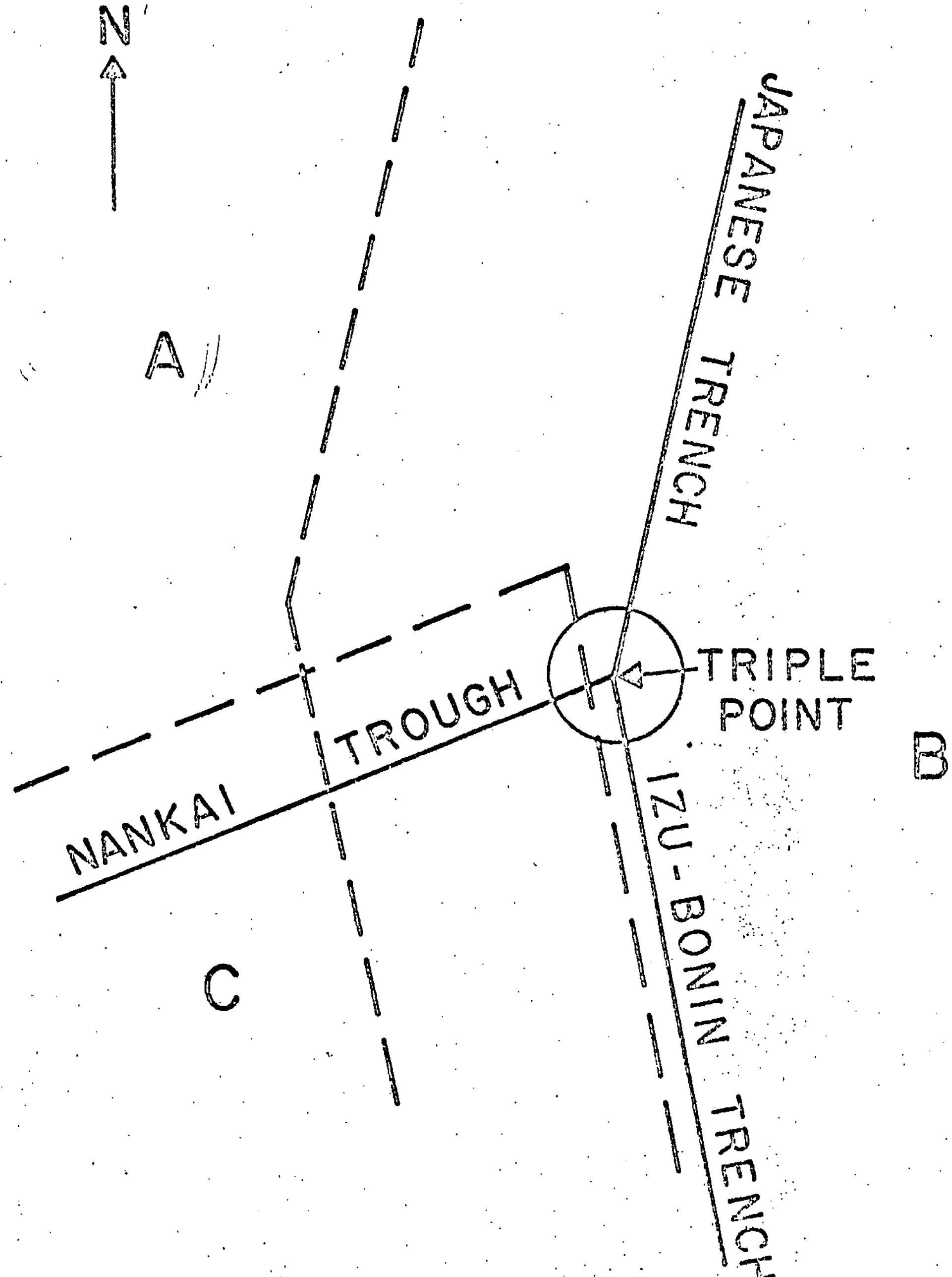

SLIP VECTOR	RATE cm/yr	STRIKE
AB	22	W 13° N
AC	8	W 6° S
BC	17	N 20° W

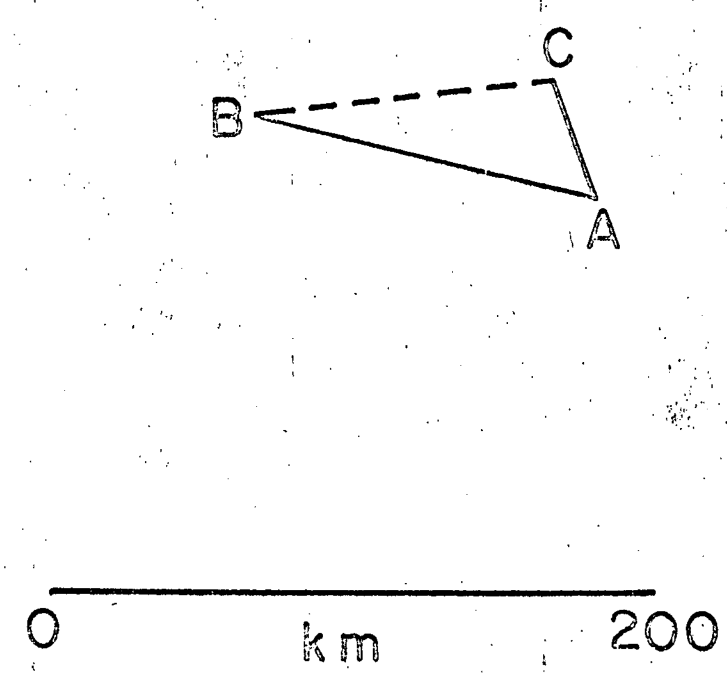

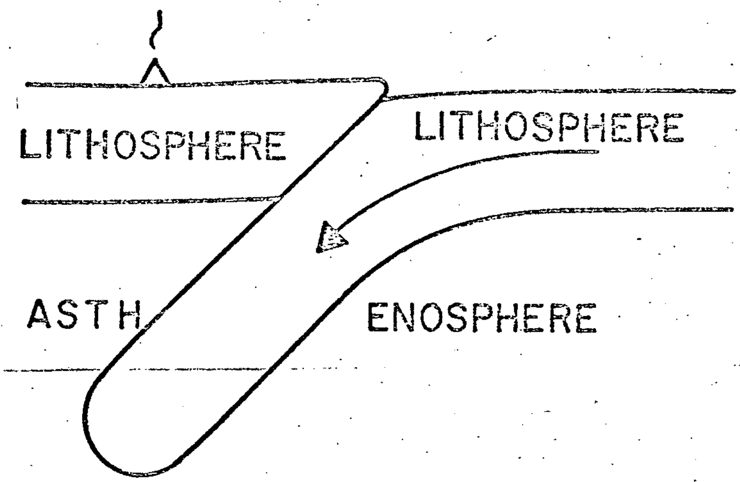

PRE-SEISMIC

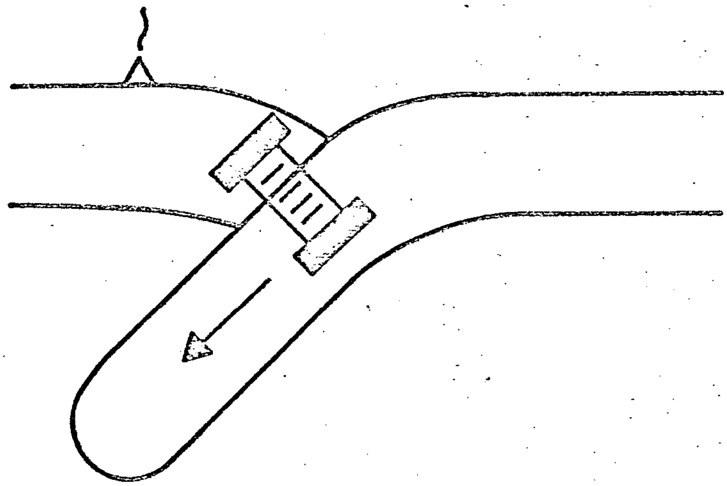

SEISMIC